

5-HT release in nucleus accumbens rescues social deficits in mouse autism model

Jessica J. Walsh¹, Daniel J. Christoffel¹, Boris D. Heifets², Gabriel A. Ben-Dor¹, Aslihan Selimbeyoglu^{1,3,4}, Lin W. Hung¹, Karl Deisseroth^{3,4} & Robert C. Malenka^{1*}

Dysfunction in prosocial interactions is a core symptom of autism spectrum disorder. However, the neural mechanisms that underlie sociability are poorly understood, limiting the rational development of therapies to treat social deficits. Here we show in mice that bidirectional modulation of the release of serotonin (5-HT) from dorsal raphe neurons in the nucleus accumbens bidirectionally modifies sociability. In a mouse model of a common genetic cause of autism spectrum disorder—a copy number variation on chromosome 16p11.2—genetic deletion of the syntenic region from 5-HT neurons induces deficits in social behaviour and decreases dorsal raphe 5-HT neuronal activity. These sociability deficits can be rescued by optogenetic activation of dorsal raphe 5-HT neurons, an effect requiring and mimicked by activation of 5-HT_{1b} receptors in the nucleus accumbens. These results demonstrate an unexpected role for 5-HT action in the nucleus accumbens in social behaviours, and suggest that targeting this mechanism may prove therapeutically beneficial.

Positive prosocial interactions contribute to the development and maintenance of a range of adaptive, cooperative behaviours. Conversely, abnormal social interactions are debilitating symptoms of several neuropsychiatric disorders, notably autism spectrum disorder (ASD)^{1,2}. Although the role of neuromodulators in social behaviours, in particular oxytocin, is an active area of investigation, relatively little is known about the neural mechanisms that influence sociability. Activation of oxytocin receptors on 5-HT terminals in the nucleus accumbens (NAc) is essential for the processing of social rewards³, raising the possibility that 5-HT release in the NAc contributes to prosocial interactions. The serotonergic system has long been implicated in behavioural deficits associated with psychiatric disorders^{4,5}, with some findings suggesting that changes in brain levels of 5-HT or manipulations of 5-HT signalling can influence social behaviours^{6–10}. Indeed, an early clue for a role of 5-HT in social behaviour came from measuring abnormal blood 5-HT levels in children with autism¹¹.

Here, we directly test the hypothesis that bidirectional modulation of 5-HT release in the NAc bidirectionally modifies sociability. We study the importance of this mechanism for ASD by examining a mouse model of copy number variations on human chromosome 16p11.2, a common genetic variation associated with ASD^{12–14}. Deletion of chromosome 7F3, which is syntenic to human 16p11.2, specifically from 5-HT neurons induced deficits in social behaviour, decreased dorsal raphe (DR) 5-HT activity during social contact, and reduced DR 5-HT neuron excitability. The decrease in sociability in 16p11.2 deletion mice was rescued by activation of DR 5-HT neurons, an effect requiring NAc 5-HT_{1b} receptors. Similar rescue of social behaviour deficits was achieved by pharmacological activation of NAc 5-HT_{1b} receptors. These results establish the importance of 5-HT action in the NAc in prosocial behaviours and suggest a rational path for the development of new therapeutic agents for the treatment of social behaviour deficits in neuropsychiatric disorders.

NAc 5-HT terminal activity influences sociability

We examined how DR neuron activity regulates social behaviour by injecting adeno-associated viruses (AAV) expressing channelrhodopsin-2

fused to enhanced yellow fluorescent protein (ChR2–eYFP) or eYFP alone into the DR of wild-type mice implanted with an optic fibre above the DR (Fig. 1a). Sociability was assayed by juvenile interaction and three-chamber tests along with open field locomotion and novel object interaction assays (Fig. 1b). Activation of DR neurons expressing ChR2 (at 20 Hz) caused increases in sociability in both assays, whereas no effects were observed in eYFP-expressing control mice that received light stimulation (Fig. 1c, d; Extended Data Fig. 1a, b). DR neuron activation had no effect on control behaviours (Fig. 1e, f) or anxiety-related behaviours (Extended Data Fig. 1c). Importantly, all assays were conducted and analysed in a blinded fashion.

The NAc contributes to the regulation of social behaviours^{3,15–19}. To determine whether the NAc was a crucial target of the activated DR neurons, we injected AAVs into the DR of wild-type mice and implanted optic fibres bilaterally above the NAc (Fig. 1g). Activation of DR terminals in the NAc expressing ChR2 caused increases in both sociability assays, whereas control mice exhibited no change in sociability (Fig. 1h–j; Extended Data Fig. 1d, e). Terminal activation of neurons projecting from the DR to the NAc did not influence the novel object interaction assay, locomotor activity or anxiety-related behaviours (Fig. 1k, l; Extended Data Fig. 1f).

5-HT is implicated in the regulation of social behaviours^{3,6–11} and a major source is DR 5-HT neurons²⁰. To test whether modulation of DR 5-HT neuron activity alters sociability, we injected double-floxed AAV-DIO-ChR2–eYFP (DIO-ChR2) or AAV-DIO-NpHR–eYFP (DIO-NpHR), which expresses the inhibitory opsin NpHR3.0, into the DR of mice that express Cre specifically in 5-HT neurons (*Sert-cre*, also known as *Slc6a4-cre*, mice)²¹ and implanted optic fibres above the DR (Fig. 2a, b). *Sert-cre* mice injected with AAV-DIO–eYFP served as controls. Optogenetic activation of DR 5-HT neurons increased sociability (Fig. 2c, d; Extended Data Fig. 1g, h), whereas optogenetic inhibition of DR 5-HT neurons decreased sociability (Fig. 2e, f; Extended Data Fig. 1i, j). Control mice were unaffected by light stimulation (Fig. 2c–f; Extended Data Fig. 1g–j) and control behaviours were unaffected by manipulation of DR 5-HT neuron activity (Extended Data Fig. 1k–p).

¹Nancy Pritzker Laboratory, Department of Psychiatry and Behavioral Sciences, Stanford University, Stanford, CA, USA. ²Department of Anesthesiology, Perioperative and Pain Medicine, Stanford University School of Medicine, Stanford, CA, USA. ³Howard Hughes Medical Institute, Stanford University, Stanford, CA, USA. ⁴Department of Bioengineering and Department of Psychiatry and Behavioral Sciences, Stanford University, Stanford, CA, USA. *e-mail: malenka@stanford.edu

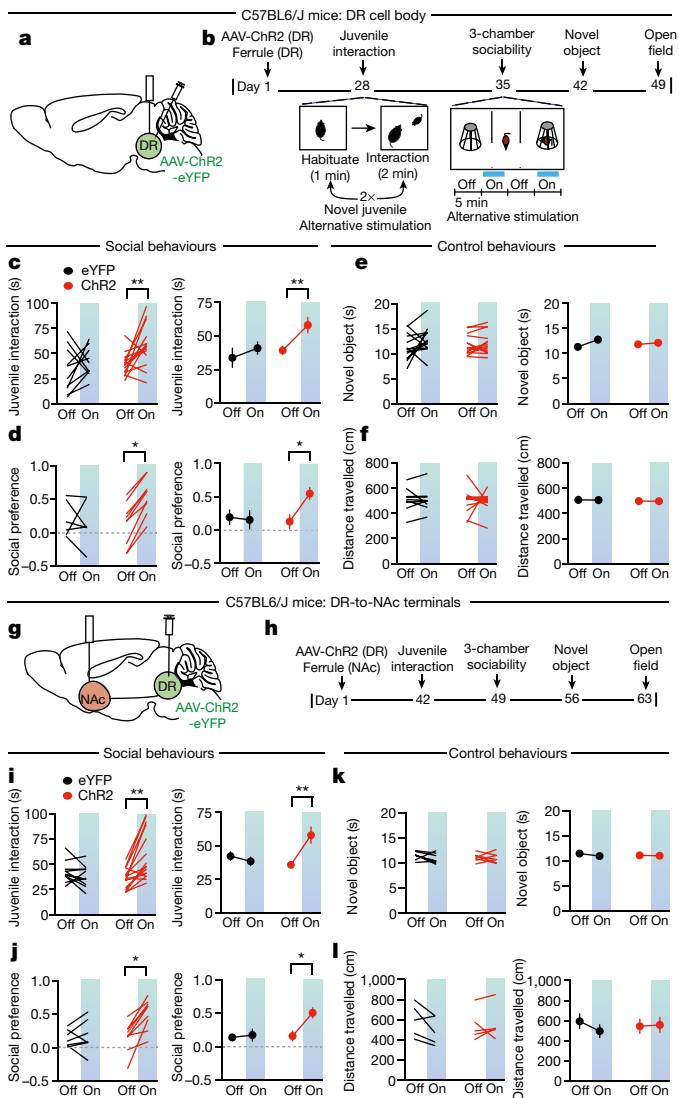


Fig. 1 | Activation of DR neurons or their NAc projections increases sociability. **a**, Schematic of optogenetic manipulation. **b**, Timeline of experiments. **c**, **d**, Quantification of juvenile interaction assay (**c**: $F_{1,44} = 6.262$, $P < 0.05$; $n = 10-14$) and three-chamber sociability assay (**d**: $F_{1,26} = 4.327$, $P < 0.05$; $n = 6-9$) in wild-type mice (blue signifies optical activation). In this and all subsequent figures, the left panels illustrate individual subjects; right panels display mean \pm s.e.m. **e**, **f**, DR neuron stimulation did not alter the novel object interaction assay (**e**: $F_{1,52} = 0.8324$, $P = 0.3658$, $n = 14$) or the locomotion assay (**f**: $F_{1,44} = 0.00053$, $P = 0.9817$; $n = 10-14$). **g**, Schematic of optogenetic manipulation. **h**, Timeline of experiments. **i**, **j**, Quantification of juvenile interaction (**i**: $F_{1,50} = 8.999$, $P < 0.01$; $n = 11-16$) and three-chamber sociability (**j**: $F_{1,28} = 4.320$, $P < 0.05$; $n = 7-9$) assays in wild-type mice. **k**, **l**, Stimulation of DR-to-NAc terminals does not alter the novel object interaction assay (**k**: $F_{1,24} = 0.4047$, $P = 0.5307$, $n = 7$) or the locomotion assay (**l**: $F_{1,16} = 0.6484$, $P = 0.4325$, $n = 5$). * $P < 0.05$, ** $P < 0.01$; two-way ANOVA with Tukey's multiple comparison post hoc test. Comparisons with no asterisk had $P > 0.05$ and were considered not significant. The schematic of the mouse brain in this figure has been adapted with permission from Franklin & Paxinos⁴⁶.

To test whether modifying 5-HT terminal activity in the NAc specifically recapitulates the consequences of DR 5-HT somatic manipulations, we expressed DIO-ChR2 or DIO-NpHR in the DR of *Sert-cre* mice and implanted optic fibres in the NAc (Fig. 2g, h). Identical to somatic stimulation, terminal activation of 5-HT neurons projecting from the DR to the NAc increased sociability (Fig. 2i, j; Extended Data Fig. 2a, b), whereas inhibition substantially decreased sociability (Fig. 2k, l; Extended Data Fig. 2c, d) with no effects in control mice

(Fig. 2i–l; Extended Data Fig. 2a–d) and no effects of ChR2 or NpHR activation on the novel object interaction assay, locomotor activity, or anxiety-related behaviours (Extended Data Fig. 2e–j).

Effects of 16p11.2 deletion in DR 5-HT neurons

Abnormalities in the brain's 5-HT system are implicated in ASD^{7,10,11,22}, providing motivation to test the relevance of our findings to ASD pathophysiology. We studied a mouse model of the 16p11.2 deletion syndrome because this is a common genetic variation associated with ASD^{12–14} and a floxed mouse line (*16p11.2^{flx}*) was available²³, allowing for control over deletion of the syntenic region on mouse chromosome 7F3 (Fig. 3a). We first examined whole brain 16p11.2 deletion by crossing *16p11.2^{flx}* mice to a *Nes-creER* mouse line (*16p11.2^{flx}:Nes-creER*), which limits Cre expression to neurons and is tamoxifen dependent allowing for temporal control of the genetic deletion²⁴ (Fig. 3b, c). Homozygous *16p11.2^{flx}:Nes-creER* mice exhibited decreased sociability, whereas heterozygous mice exhibited a decrease in juvenile interactions and a trend towards a decrease in three-chamber assays (Fig. 3d, e; Extended Data Fig. 3a, b). Neither group of 16p11.2 deletion mice exhibited changes in the novel object interaction assay (Fig. 3f), whereas homozygous *16p11.2^{flx}:Nes-creER* mice exhibited hyperactivity (Fig. 3g), as observed previously^{23,25}. None of the groups exhibited changes in anxiety-related behaviours in the open field test (Extended Data Fig. 3c).

To examine 16p11.2 deletion specifically in DR neurons as well as isolate the deletion solely to 5-HT neurons, we infused AAV-DJ-Cre²⁶ into the DR of *16p11.2^{flx}* mice (Fig. 3h) or crossed *Sert-cre* mice to floxed mice (*Sert-cre:16p11.2^{flx}*) (Fig. 3i, j). Both *16p11.2^{flx}* mice expressing Cre in the DR and *Sert-cre:16p11.2^{flx}* mice exhibited decreases in sociability compared to *16p11.2^{flx}* mice that had control AAV-DJ- Δ Cre infused into DR (Fig. 3k, l; Extended Data Fig. 3d, e), with no abnormalities in the novel object interaction assay, locomotion, or anxiety-related behaviours (Fig. 3m, n; Extended Data Fig. 3f).

To assess DR 5-HT neuron activity during social interaction, *Sert-cre* and *Sert-cre:16p11.2^{flx}* mice were infused with AAV-DJ-DIO-GCaMP6f into the DR and fibre optics implanted above DR to perform fibre photometry recordings (Fig. 4a). DR 5-HT neuron activity increased during social interaction in *Sert-cre* mice⁹ and the magnitude of this increase was reduced in mice with 16p11.2 deleted from 5-HT neurons (Fig. 4b, c). To further assess how 16p11.2 deletion affects the function of DR 5-HT neurons, *Sert-cre* and *Sert-cre:16p11.2^{flx}* mice were injected with DIO-eYFP into the DR so that we could make whole-cell recordings from identified 5-HT neurons in acute DR slices. DR 5-HT neurons lacking 16p11.2 exhibited a decrease in spiking in response to depolarizing current pulses (Fig. 4d, e). These neurons also exhibited an approximately 50% decrease in the amplitude of spontaneous excitatory postsynaptic currents (Fig. 4f, g) with no change in their frequency (Fig. 4h, i). These results suggest that DR 5-HT neuron spiking is reduced after deletion of 16p11.2 and that impairment of DR 5-HT neuron activity contributes to the behavioural deficits observed in 16p11.2 deletion mice.

NAc 5-HT rescues social deficits in 16p11.2^{flx} mice

If sociability deficits in 16p11.2 deletion mice are due to reduced function of DR 5-HT neurons, it may be possible to rescue the deficits by driving DR 5-HT neuron activity. To test this prediction, we infused AAV-DJ-Cre and either DIO-ChR2 or DIO-eYFP into the DR of *16p11.2^{flx}* mice to express these transgenes in DR neurons lacking 16p11.2 and implanted an optic fibre above the DR (Extended Data Fig. 4a, b). As expected (Fig. 3k, l), eYFP mice displayed decreased sociability, whereas optogenetic activation of DR neurons rescued these sociability deficits (Extended Data Fig. 4c–f) with no changes in control behaviours (Extended Data Fig. 4g–i).

To determine whether 5-HT neuron activation specifically is sufficient to reverse the sociability deficits caused by 16p11.2 deletion, *Sert-cre:16p11.2^{flx}* mice were injected with DIO-ChR2 or DIO-eYFP. Activation of DR 5-HT neurons rescued the social behaviour deficits

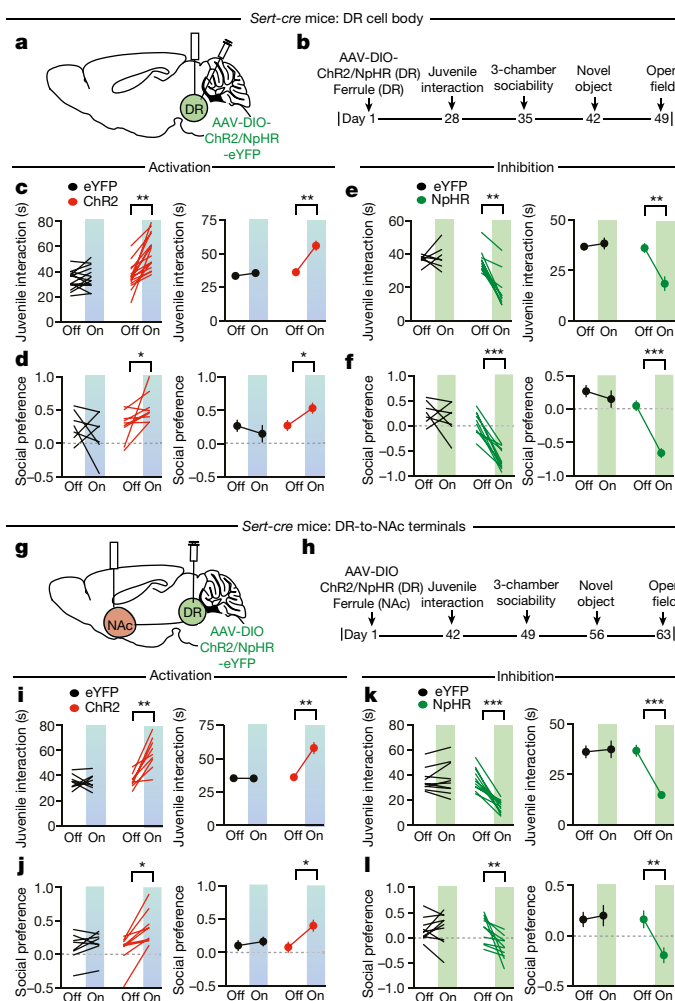


Fig. 2 | Bidirectional modulation of DR 5-HT neuron activity modifies sociability. **a**, Schematic of optogenetic manipulation. **b**, Timeline of experiments. **c**, **d**, Quantification of juvenile interaction (**c**: $F_{1,56} = 10.85$, $P < 0.01$; $n = 14-16$) and three-chamber sociability (**d**: $F_{1,28} = 4.597$, $P < 0.05$; $n = 7-9$) assays in *Sert-cre* mice expressing Chr2 or eYFP. **e**, **f**, Quantification of juvenile interaction (**e**: $F_{1,30} = 12.77$, $P < 0.01$; $n = 7-10$) and three-chamber sociability (**f**: $F_{1,30} = 11.98$, $P < 0.001$; $n = 7-10$) assays in *Sert-cre* mice expressing NpHR or eYFP. **g**, Schematic of optogenetic manipulation. **h**, Timeline of experiments. **i**, **j**, Quantification of juvenile interaction (**i**: $F_{1,30} = 15.78$, $P < 0.01$; $n = 8-9$) and three-chamber sociability (**j**: $F_{1,30} = 6.413$, $P < 0.05$; $n = 8-9$) in *Sert-cre* mice expressing Chr2 or eYFP. **k**, **l**, Quantification of juvenile interaction (**k**: $F_{1,38} = 16.29$, $P < 0.001$; $n = 10-11$) and three-chamber sociability (**l**: $F_{1,36} = 5.66$, $P < 0.01$; $n = 10$) assays in *Sert-cre* mice expressing NpHR or eYFP. Data are mean \pm s.e.m. * $P < 0.05$, ** $P < 0.01$, *** $P < 0.001$; two-way ANOVA with Tukey's multiple comparison post hoc test. Comparisons with no asterisk had $P > 0.05$ and were considered not significant. The schematic of the mouse brain in this figure has been adapted with permission from Franklin & Paxinos⁴⁶.

in mice with 16p11.2 deletion from 5-HT neurons (Fig. 5a, b; Extended Data Fig. 5a, b) while this manipulation again had no effect on the novel object interaction assay, locomotion or anxiety-related behaviours (Extended Data Fig. 5c-e). To determine whether enhancing 5-HT release specifically in the NAc would have the same effects, we repeated these manipulations but placed the optic fibres in the NAc. Activation of DR-to-NAc 5-HT terminals rescued the sociability deficits in mice with 16p11.2 deletion from 5-HT neurons (Fig. 5c, d; Extended Data Fig. 5f, g) and had no effect on control behaviours (Extended Data Fig. 5h-j). Dopamine release in the NAc also enhances social interaction¹⁷ but is strongly reinforcing on its own²⁷⁻³⁰. To examine whether 5-HT release in the NAc shares these features, we performed two assays: real-time

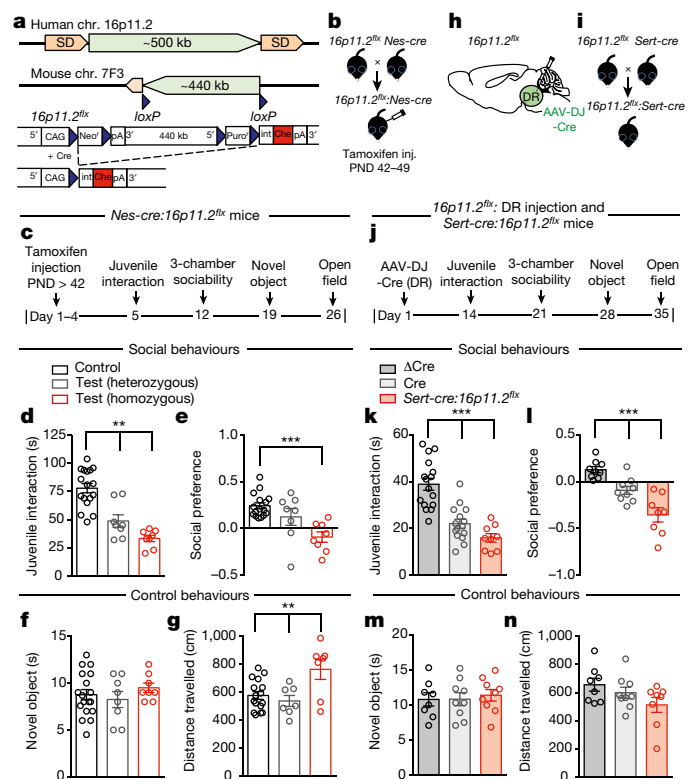


Fig. 3 | 16p11.2 deletion in DR and 5-HT neurons decreases sociability. **a**, Schematic of human chromosome 16p11.2 and deletion of syntenic region of mouse chromosome 7F3. **b**, Genetic crosses used to delete 16p11.2 from whole brain. PND, postnatal day. **c**, Timeline of experiments. **d**, **e**, Quantification of juvenile interaction (**d**: $F_{2,30} = 26.98$, $P < 0.01$; $n = 8-17$) and three-chamber sociability (**e**: $F_{2,29} = 10.03$, $P < 0.001$; $n = 8-16$) in control, heterozygous and homozygous mice with deletion of 16p11.2. **f**, **g**, Deletion of 16p11.2 does not alter the novel object interaction assay (**f**: $F_{2,31} = 0.6613$, $P = 0.5233$; $n = 8-18$) but homozygous 16p11.2 deletion increases locomotor activity (**g**: $F_{2,27} = 6.341$, $P < 0.01$; $n = 7-16$). **h**, Schematic of 16p11.2 deletion in DR. **i**, Genetic crosses to delete 16p11.2 from 5-HT neurons. **j**, Timeline of experiments. **k**, **l**, Quantification of juvenile interaction (**k**: $F_{2,37} = 26.72$, $P < 0.001$; $n = 9-16$) and three-chamber sociability (**l**: $F_{2,23} = 21.45$, $P < 0.001$; $n = 8-9$) assays in 16p11.2^{flx} mice expressing Δ Cre or Cre in DR and *Sert-cre:16p11.2^{flx}* mice. **m**, **n**, Deletion of 16p11.2 did not alter the novel object interaction assay (**m**: $F_{2,23} = 0.138$, $P = 0.8718$, $n = 8-9$) or the locomotion assay (**n**: $F_{2,22} = 2.371$, $P = 0.1168$, $n = 8-9$). Data are mean \pm s.e.m. ** $P < 0.01$; *** $P < 0.001$; one-way ANOVA with Tukey's multiple comparison post hoc test. The schematic of the mouse brain in this figure has been adapted with permission from Franklin & Paxinos⁴⁶.

conditioned placed preference (CPP) and optogenetic intracranial self-stimulation. Optogenetic activation of DR-to-NAc 5-HT inputs did not elicit real-time CPP or nose poking for stimulation in the optogenetic intracranial self-stimulation protocol in either *Sert-cre* or *Sert-cre:16p11.2^{flx}* mice (Extended Data Fig. 6a-e). These results suggest that 5-HT release in the NAc, unlike dopamine release, is not acutely reinforcing.

To assess the specificity of 5-HT action in the NAc, we asked whether activation of 5-HT inputs to the NAc enhanced interactions with a non-social appetitive stimulus by performing a three-chamber test during which a high-fat food pellet was placed in one chamber. Control *Sert-cre* mice spent more time in the chamber containing the food pellet, confirming that it was appetitive, but activation of 5-HT inputs in the NAc did not increase preference for this food chamber (Extended Data Fig. 6f). Similar negative results were obtained in *Sert-cre:16p11.2^{flx}* mice (Extended Data Fig. 6g). To address whether 5-HT release in brain regions other than the NAc influences sociability, we activated 5-HT terminals in the dorsal striatum, a site that subserves

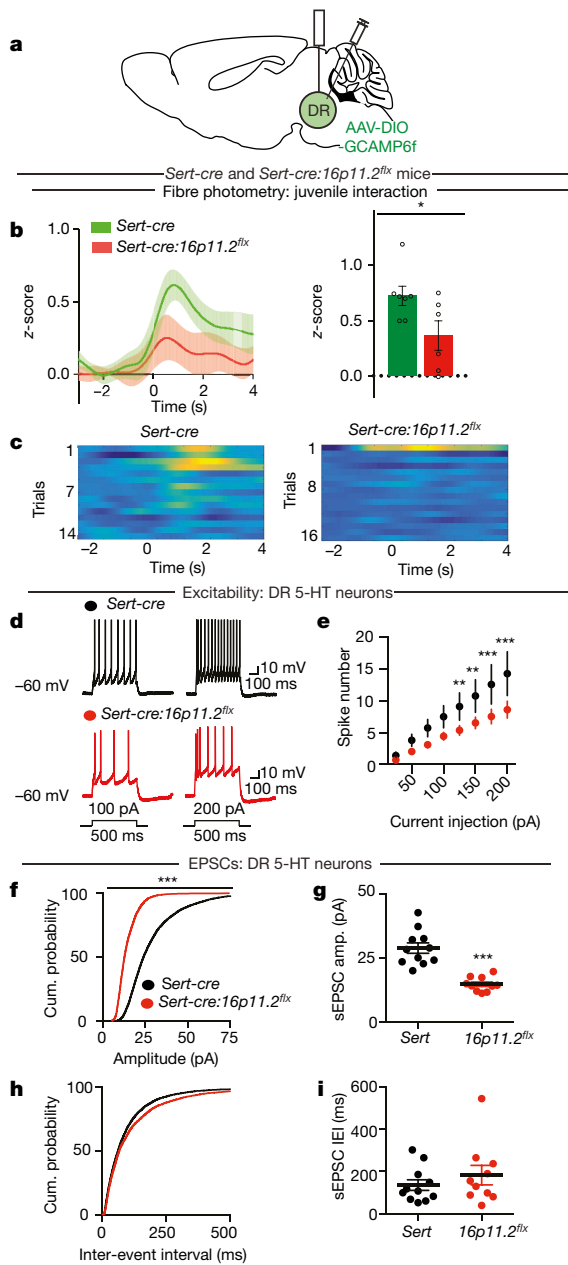


Fig. 4 | 16p11.2 deletion in DR 5-HT neurons decreases their activity. **a**, Schematic of experimental set-up. **b**, Left, time course of average GCaMP6f transient z-scores event-locked to social interaction. Right, quantification of average peak z-score during social interaction ($t_{11} = 2.321, P < 0.05$). **c**, Representative heat map of z-score changes over all trials from single mice. **d**, Sample traces of spiking in 5-HT DR neurons. **e**, Quantification of spiking ($F_{7,56} = 2.305, P < 0.05$). **f**, Summary of cumulative probability of spontaneous excitatory postsynaptic current (sEPSC) amplitudes. **g**, Mean sEPSC amplitude changes ($t_{19} = 0.069, P < 0.001, n = 10-11$). **h**, Summary of cumulative probability of sEPSC frequency. **i**, Mean sEPSC frequency changes. * $P < 0.05$, ** $P < 0.01$, *** $P < 0.001$; unpaired t -test (**b, g, i**), repeated measures two-way ANOVA with Sidak's multiple comparison post hoc test (**d**), or Kolmogorov-Smirnov test (**f, h**). The schematic of the mouse brain in this figure has been adapted with permission from Franklin & Paxinos⁴⁶.

different functions from the NAc³¹⁻³⁴. Activation of DR 5-HT terminals in the dorsal striatum had no effect in the sociability assays (Extended Data Fig. 7a-f) or in the novel object interaction assay or locomotion in the open field (Extended Data Fig. 7g, h). However, 5-HT terminal activation in dorsal striatum did cause a decrease in the open field centre time in *Sert-cre* mice (Extended Data Fig. 7i), demonstrating the stimulation was effective.

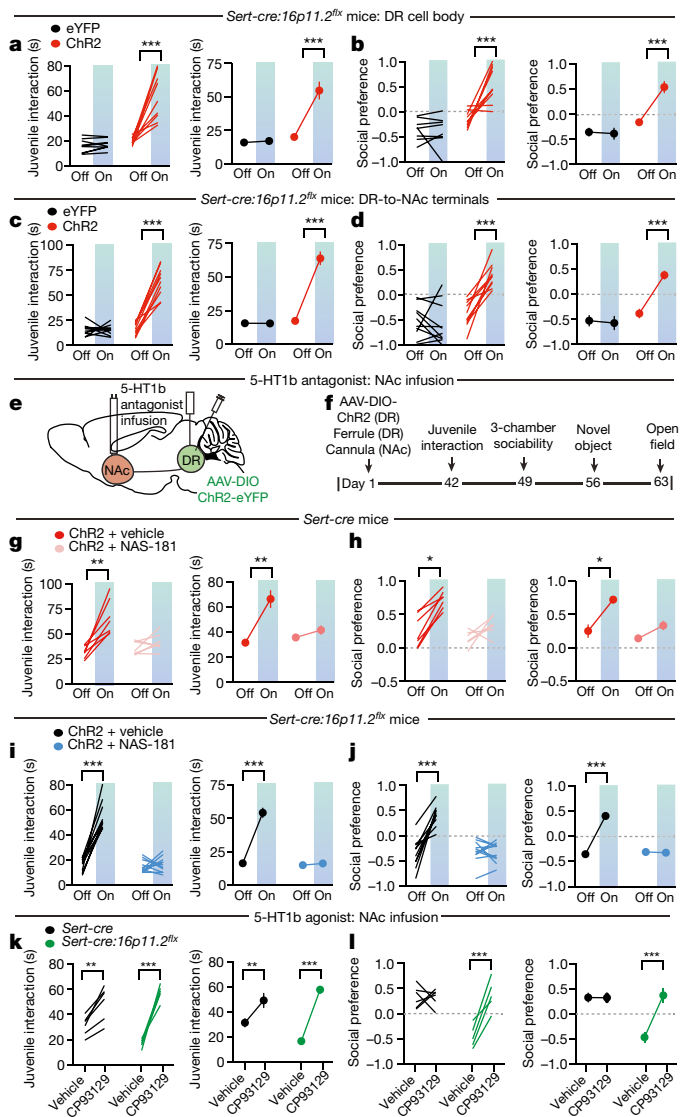


Fig. 5 | Rescue of social deficits in 16p11.2 deletion mice by 5-HT activity in the NAc. **a, b**, Quantification of juvenile interaction (**a**: $F_{1,32} = 25.15, P < 0.001; n = 9$) and three-chamber sociability (**b**: $F_{1,32} = 16.63, P < 0.001; n = 8-10$) assays in *Sert-cre:16p11.2flx* mice expressing Chr2 or eYFP receiving soma stimulation. **c, d**, Quantification of juvenile interaction (**c**: $F_{1,36} = 69.84, P < 0.001; n = 10$) and three-chamber sociability (**d**: $F_{1,36} = 16.46, P < 0.001; n = 10$) assays in *Sert-cre:16p11.2flx* mice expressing Chr2 or eYFP receiving DR-to-NAc terminal stimulation. **e**, Schematic of experimental set-up. **f**, Timeline of experiments. **g, h**, Quantification of juvenile interaction (**g**: $F_{1,24} = 12.6, P < 0.01; n = 7$) and three-chamber sociability (**h**: $F_{1,22} = 4.322, P < 0.05; n = 7$) in *Sert-cre* mice expressing Chr2 in DR with either vehicle or NAS-181 infused into NAc. **i, j**, Quantification of juvenile interaction (**i**: $F_{1,40} = 29.24, P < 0.001; n = 11$) and three-chamber sociability (**j**: $F_{1,38} = 29.06, P < 0.001; n = 10-11$) in *Sert-cre:16p11.2flx* mice expressing Chr2 in DR with either vehicle or NAS-181 infused into NAc. **k, l**, Quantification of juvenile interaction (**k**: $F_{1,9} = 19.03, P < 0.001; n = 10-11$) and three-chamber sociability (**l**: $F_{1,9} = 18.4, P < 0.01; n = 5-6$) in *Sert-cre* and *Sert-cre:16p11.2flx* mice with either vehicle or CP93129 infused into NAc. Data are mean \pm s.e.m. * $P < 0.05$, ** $P < 0.01$, *** $P < 0.001$; two-way ANOVA with Sidak's multiple comparison post hoc test. The schematic of the mouse brain in this figure has been adapted with permission from Franklin & Paxinos⁴⁶.

A question with therapeutic implications is whether the enhancement of sociability caused by the activation of DR-to-NAc 5-HT terminals outlasts the stimulation. To address this topic, we activated DR-to-NAc 5-HT terminals in *Sert-cre* and *Sert-cre:16p11.2flx* mice on

several days. Although stimulation on day 1 caused robust increases in sociability (Extended Data Fig. 8a), there was no lasting effect when these mice were assayed the next day even though they again showed an acute enhancement of sociability during stimulation (Extended Data Fig. 8b). To assess whether more prolonged terminal stimulation of DR-to-NAc 5-HT neurons could elicit effects beyond the stimulation period, we performed stimulation assays four times with 2 h between sessions on days 3 and 4: mice thereby received 10 bouts of DR-to-NAc 5-HT terminal stimulation over 4 days. Mice consistently showed enhanced sociability during each stimulation bout, but no carry over effects were observed (Extended Data Fig. 8c–j).

Role of NAc 5-HT1b receptors in enhanced sociability

Blockade of 5-HT1b receptors in the NAc abolishes the reinforcing properties of social interaction in a CPP assay³. To test whether the effects of DR 5-HT neuron activation on sociability also require NAc 5-HT1b receptors, we infused a 5-HT1b receptor antagonist (NAS-181) into the NAc before optogenetic behavioural assays in *Sert-cre* mice (Fig. 5e, f). As expected (Fig. 2c, d), the activation of DR 5-HT neurons caused increases in sociability, which were blocked by NAS-181 infusions into the NAc (Fig. 5g, h; Extended Data Fig. 9a, b). Identical NAc infusions of NAS-181 had no effects on sociability assays in control *Sert-cre* mice expressing eYFP (Extended Data Fig. 9c–f) nor on control behaviours in any of the cohorts of mice (Extended Data Figs. 9g–i, 10a–c). We next examined whether the rescue of sociability deficits by DR 5-HT neuron stimulation in mice with 16p11.2 deletion was also dependent on NAc 5-HT1b receptors. The increase in sociability elicited by DR 5-HT neuron activation was again observed in *Sert-cre:16p11.2^{flx}* mice that received NAc infusions of vehicle, and these behavioural effects were prevented by infusions of NAS-181 (Fig. 5i, j; Extended Data Fig. 10d, e) with no effects on control behaviours in either cohort of mice (Extended Data Fig. 10f–h).

In final experiments, we asked whether pharmacological activation of NAc 5-HT1b receptors was sufficient to rescue the social deficits in 16p11.2 deletion mice. Both *Sert-cre* and *Sert-cre:16p11.2^{flx}* mice exhibited an increase in sociability during the juvenile interaction assay after direct infusion of the 5-HT1b receptor agonist CP93129 into the NAc (Fig. 5k). During the three-chamber social preference assay, NAc infusion of CP93129 robustly rescued the behavioural deficits in *Sert-cre:16p11.2^{flx}* mice while having no detectable effect in control *Sert-cre* mice (Fig. 5l, Extended Data Fig. 11a–f). Control behaviours in both cohorts of mice were unaffected by this drug treatment (Extended Data Fig. 11g–i).

Concluding remarks

Our results demonstrate that stimulating 5-HT release in the NAc promotes sociability, effects that require activation of NAc 5-HT1b receptors. Inhibition of DR 5-HT neurons or their terminals in the NAc reduced social interactions, suggesting that 5-HT action in the NAc is necessary for normal levels of sociability. Consistent with this conclusion, increases in DR 5-HT neuron activity occur during non-aggressive social interactions, including mating, although increases may also occur during sucrose or food intake⁷. Stimulating 5-HT release in the NAc did not elicit acute reinforcement or changes in a variety of control behaviours. These behavioural effects of 5-HT in the NAc are markedly different from the acute reinforcing properties of the release of dopamine in the NAc^{27–30}, suggesting critical differences in the NAc circuitry modulation by which these major neuromodulators mediate their behavioural effects.

The findings that genetic deletion of 16p11.2 specifically from 5-HT neurons caused sociability deficits accompanied by decreases in DR 5-HT neuron activity during social interactions as well as in vitro electrophysiological assays provide further evidence for the importance of DR 5-HT neuron activity in prosocial behaviours. However, further work is necessary to determine how accurately the postnatal, spatially restricted homozygous deletion of 16p11.2 in mice mimics the human heterozygous deletion syndrome and whether other autism models

will express deficits in DR 5-HT neuron functioning. The rescue of sociability deficits by DR 5-HT neuron activation raises the question of whether drugs that influence 5-HT levels are beneficial in treating ASD. Serotonin reuptake inhibitors treat anxiety and obsessive-compulsive behaviours associated with ASD with variable efficacy, but there is little evidence that they ameliorate social deficits³⁵. Our results demonstrate that direct activation of NAc 5-HT1b receptors or increased 5-HT release in the NAc is sufficient to ameliorate social deficits. Unlike the optogenetic inhibition of 5-HT neuron activity (Fig. 2), however, NAc infusion of the 5-HT1b receptor antagonist did not impair baseline sociability (Fig. 5). These results suggest that the influence of 5-HT in the NAc on sociability probably involves other subtypes of 5-HT receptor.

Another potential pharmacological intervention for promoting sociability is MDMA (3,4-methylenedioxymethamphetamine), which robustly releases 5-HT in an activity-independent manner and is being tested for its therapeutic utility³⁶. Optogenetic stimulation of DR 5-HT neurons is more likely to mimic the effects of MDMA on 5-HT levels in target structures, than serotonin reuptake inhibitors. Thus, like dopamine³⁷, the behavioural effects of drugs that influence 5-HT uptake or release probably depend on the specific influence of the drug on 5-HT levels and kinetics.

The DR is a heterogenous structure that contains several cell types. Previous studies suggest that manipulations of the activity of these cells have complex effects on motivated behaviours^{9,38–45}. Assuming that the large body of work on dopamine modulation of target circuits and behaviours is an appropriate comparator^{27–30}, 5-HT modulation of circuits and behaviours will be equally complex and depend on its specific anatomical targets. Our findings suggest that detailed exploration of 5-HT function using modern circuit neuroscience tools will not only advance our understanding of the adaptive role of this neuromodulatory system but will also provide insights that will prove valuable for development of mechanistically novel therapies for the treatment of prevalent neuropsychiatric disorders such as ASD.

Online content

Any Methods, including any statements of data availability and Nature Research reporting summaries, along with any additional references and Source Data files are available in the online version of the paper at <https://doi.org/10.1038/s41586-018-0416-4>.

Received: 22 June 2017; Accepted: 27 June 2018;

Published online: 08 August 2018

- Christensen, D. L. et al. Prevalence and characteristics of autism spectrum disorder among children aged 8 years—autism and developmental disabilities monitoring network, 11 Sites, United States, 2012. *MMWR Surveill. Summ.* **65**, 1–23 (2016).
- Chevallier, C., Kohls, G., Troiani, V., Brodtkin, E. S. & Schultz, R. T. The social motivation theory of autism. *Trends Cogn. Sci.* **16**, 231–239 (2012).
- Dölen, G., Darvishzadeh, A., Huang, K. W. & Malenka, R. C. Social reward requires coordinated activity of nucleus accumbens oxytocin and serotonin. *Nature* **501**, 179–184 (2013).
- Brown, S.-L. & Praag, H. M. v. *The Role of Serotonin in Psychiatric Disorders* (Brunner/Mazel, New York, 1991).
- Charney, D. S., Sklar, P. B., Buxbaum, J. D. & Nestler, E. J. *Charney & Nestler's Neurobiology of Mental Illness* 5th edn (Oxford Univ. Press, 2018).
- Furray, A. R., McDevitt, R. A., Miczek, K. A. & Neumaier, J. F. 5-HT1B mRNA expression after chronic social stress. *Behav. Brain Res.* **224**, 350–357 (2011).
- Kane, M. J. et al. Mice genetically depleted of brain serotonin display social impairments, communication deficits and repetitive behaviors: possible relevance to autism. *PLoS One* **7**, e48975 (2012).
- Challis, C. et al. Raphe GABAergic neurons mediate the acquisition of avoidance after social defeat. *J. Neurosci.* **33**, 13978–13988, 13988a (2013).
- Li, Y. et al. Serotonin neurons in the dorsal raphe nucleus encode reward signals. *Nat. Commun.* **7**, 10503 (2016).
- Muller, C. L., Anacker, A. M. J. & Veenstra-VanderWeele, J. The serotonin system in autism spectrum disorder: From biomarker to animal models. *Neuroscience* **321**, 24–41 (2016).
- Schain, R. J. & Freedman, D. X. Studies on 5-hydroxyindole metabolism in autistic and other mentally retarded children. *J. Pediatr.* **58**, 315–320 (1961).
- Weiss, L. A. et al. Association between microdeletion and microduplication at 16p11.2 and autism. *N. Engl. J. Med.* **358**, 667–675 (2008).
- Kumar, R. A. et al. Recurrent 16p11.2 microdeletions in autism. *Hum. Mol. Genet.* **17**, 628–638 (2008).

14. Sanders, S. J. et al. Multiple recurrent de novo CNVs, including duplications of the 7q11.23 Williams syndrome region, are strongly associated with autism. *Neuron* **70**, 863–885 (2011).
15. Christoffel, D. J. et al. IKB kinase regulates social defeat stress-induced synaptic and behavioral plasticity. *J. Neurosci.* **31**, 314–321 (2011).
16. Walsh, J. J. et al. Stress and CRF gate neural activation of BDNF in the mesolimbic reward pathway. *Nat. Neurosci.* **17**, 27–29 (2014).
17. Gunaydin, L. A. et al. Natural neural projection dynamics underlying social behavior. *Cell* **157**, 1535–1551 (2014).
18. Francis, T. C. et al. Nucleus accumbens medium spiny neuron subtypes mediate depression-related outcomes to social defeat stress. *Biol. Psychiatry* **77**, 212–222 (2015).
19. Wallace, D. L. et al. CREB regulation of nucleus accumbens excitability mediates social isolation-induced behavioral deficits. *Nat. Neurosci.* **12**, 200–209 (2009).
20. Luo, M., Zhou, J. & Liu, Z. Reward processing by the dorsal raphe nucleus: 5-HT and beyond. *Learn. Mem.* **22**, 452–460 (2015).
21. Gong, S. et al. Targeting Cre recombinase to specific neuron populations with bacterial artificial chromosome constructs. *J. Neurosci.* **27**, 9817–9823 (2007).
22. Veenstra-VanderWeele, J. et al. Autism gene variant causes hyperserotonemia, serotonin receptor hypersensitivity, social impairment and repetitive behavior. *Proc. Natl Acad. Sci. USA* **109**, 5469–5474 (2012).
23. Portmann, T. et al. Behavioral abnormalities and circuit defects in the basal ganglia of a mouse model of 16p11.2 deletion syndrome. *Cell Reports* **7**, 1077–1092 (2014).
24. Burns, K. A. et al. Nestin-CreER mice reveal DNA synthesis by nonapoptotic neurons following cerebral ischemia hypoxia. *Cereb. Cortex* **17**, 2585–2592 (2007).
25. Horev, G. et al. Dosage-dependent phenotypes in models of 16p11.2 lesions found in autism. *Proc. Natl Acad. Sci. USA* **108**, 17076–17081 (2011).
26. Grimm, D. et al. *In vitro* and *in vivo* gene therapy vector evolution via multispecies interbreeding and retargeting of adeno-associated viruses. *J. Virol.* **82**, 5887–5911 (2008).
27. Tsai, H. C. et al. Phasic firing in dopaminergic neurons is sufficient for behavioral conditioning. *Science* **324**, 1080–1084 (2009).
28. Stuber, G. D., Britt, J. P. & Bonci, A. Optogenetic modulation of neural circuits that underlie reward seeking. *Biol. Psychiatry* **71**, 1061–1067 (2012).
29. Steinberg, E. E. & Janak, P. H. Establishing causality for dopamine in neural function and behavior with optogenetics. *Brain Res.* **1511**, 46–64 (2013).
30. Lammel, S., Lim, B. K. & Malenka, R. C. Reward and aversion in a heterogeneous midbrain dopamine system. *Neuropharmacology* **76 Pt B**, 351–359 (2014).
31. Steinbusch, H. W., van der Kooy, D., Verhofstad, A. A. & Pellegrino, A. Serotonergic and non-serotonergic projections from the nucleus raphe dorsalis to the caudate-putamen complex in the rat, studied by a combined immunofluorescence and fluorescent retrograde axonal labeling technique. *Neurosci. Lett.* **19**, 137–142 (1980).
32. Steinbusch, H. W. Distribution of serotonin-immunoreactivity in the central nervous system of the rat-cell bodies and terminals. *Neuroscience* **6**, 557–618 (1981).
33. Hornung, J. P. The human raphe nuclei and the serotonergic system. *J. Chem. Neuroanat.* **26**, 331–343 (2003).
34. Michelsen, K. A., Prickaerts, J. & Steinbusch, H. W. The dorsal raphe nucleus and serotonin: implications for neuroplasticity linked to major depression and Alzheimer's disease. *Prog. Brain Res.* **172**, 233–264 (2008).
35. Politte, L. C., Henry, C. A. & McDougle, C. J. Psychopharmacological interventions in autism spectrum disorder. *Harv. Rev. Psychiatry* **22**, 76–92 (2014).
36. Heifets, B. D. & Malenka, R. C. MDMA as a probe and treatment for social behaviors. *Cell* **166**, 269–272 (2016).
37. Volkow, N. D., Fowler, J. S., Wang, G. J. & Swanson, J. M. Dopamine in drug abuse and addiction: results from imaging studies and treatment implications. *Mol. Psychiatry* **9**, 557–569 (2004).
38. Qi, J. et al. A glutamatergic reward input from the dorsal raphe to ventral tegmental area dopamine neurons. *Nat. Commun.* **5**, 5390 (2014).
39. Liu, Z. et al. Dorsal raphe neurons signal reward through 5-HT and glutamate. *Neuron* **81**, 1360–1374 (2014).
40. McDevitt, R. A. et al. Serotonergic versus nonserotonergic dorsal raphe projection neurons: differential participation in reward circuitry. *Cell Reports* **8**, 1857–1869 (2014).
41. Matthews, G. A. et al. Dorsal raphe dopamine neurons represent the experience of social isolation. *Cell* **164**, 617–631 (2016).
42. Warden, M. R. et al. A prefrontal cortex-brainstem neuronal projection that controls response to behavioural challenge. *Nature* **492**, 428–432 (2012).
43. Fonseca, M. S., Murakami, M. & Mainen, Z. F. Activation of dorsal raphe serotonergic neurons promotes waiting but is not reinforcing. *Curr. Biol.* **25**, 306–315 (2015).
44. Correia, P. A. et al. Transient inhibition and long-term facilitation of locomotion by phasic optogenetic activation of serotonin neurons. *eLife* **6**, e20975 (2017).
45. Marcinkiewicz, C. A. et al. Serotonin engages an anxiety and fear-promoting circuit in the extended amygdala. *Nature* **537**, 97–101 (2016).
46. Franklin, K. B. J. & Paxinos, G. *The Mouse Brain in Stereotaxic Coordinates* 4th edn (Academic, 2012).

Acknowledgements This study was supported by the Simons Foundation Autism Research Initiative (award 305112 to R.C.M.) and NIMH (F32 MH103949 to J.J.W.).

Reviewer information Nature thanks G. Feng, M. Lobo and the other anonymous reviewer(s) for their contribution to the peer review of this work.

Author contributions J.J.W. performed the majority of experiments. D.J.C. performed the electrophysiology experiments. B.D.H. performed the fibre photometry experiments. G.A.B.-D., A.S. and L.W.H. assisted in surgeries and behavioural assays. J.J.W. and R.C.M. designed the experiments, interpreted results and wrote the paper, which was edited by all authors.

Competing interests R.C.M. and K.D. are cofounders and on the scientific advisory board of Circuit Therapeutics, Inc.

Additional information

Extended data is available for this paper at <https://doi.org/10.1038/s41586-018-0416-4>.

Supplementary information is available for this paper at <https://doi.org/10.1038/s41586-018-0416-4>.

Reprints and permissions information is available at <http://www.nature.com/reprints>.

Correspondence and requests for materials should be addressed to R.C.M.

Publisher's note: Springer Nature remains neutral with regard to jurisdictional claims in published maps and institutional affiliations.

METHODS

Experimental subjects. Male 7–9-week-old C57BL/6 mice (Jackson Laboratory), Tg(Slc6a4-cre)ET33Gsat (*Sert-cre*, Jackson Laboratory)²¹, C57BL/6-Tg(Nes-cre/Esr1*)1Kuan/J (*Nes-creER*, Jackson Laboratory)²⁴, and B6N.129P2(Cg)-Igs13^{tm1Dolm}Igs14^{tm1Dolm}/J (*16p11.2^{flx}*, gift from R. Dolmetsch, Jackson Laboratory)²³ mice were used as experimental subjects alone or following the crosses described in the text. All wild-type and *Sert-cre* mice were on C57BL/6 backgrounds. *16p11.2^{flx}* and *16p11.2^{flx}:Nes-cre* mice were on CD1 backgrounds. *Sert-cre:16p11.2^{flx}* mice were on a mixed background of C57BL/6 and CD1. In all experiments, controls were littermates on the exact same background. Juvenile mice used for the juvenile interaction assay and three-chamber sociability assay were male, conspecific and 3–5 weeks of age. Mice were housed on a 12-h light/dark cycle with food and water ad libitum. All procedures complied with the animal care standards set forth by the National Institute of Health and were approved by Stanford University's Administrative Panel on Laboratory Animal Care and Administrative Panel of Biosafety. No statistical methods were used to predetermine sample size. All experiments were conducted in a blinded manner such that assays were conducted and analysed without knowledge of the specific manipulation being performed and with animals being randomized by cage before surgery and behavioural experiments.

Viral vectors and stereotaxic surgeries for optogenetic methods. AAVs used in this study that were purchased from the University of North Carolina Viral Core included: AAV-ChR2-eYFP, AAV-eYFP, AAV-DIO-ChR2-eYFP, AAV-DIO-NpHR-eYFP, AAV-DIO-eYFP, AAV-DJ-Cre, AAV-DR-ΔCre and AAV-DJ-DIO-GCaMP6f were purchased from the Stanford Neuroscience Gene Vector and Virus Core. For surgeries, mice (7–9 weeks of age) were anaesthetized with a mixture of ketamine (100 mg kg⁻¹) and xylazine (10 mg kg⁻¹), positioned in a small-animal stereotaxic instrument (Kopf Instruments) and the skull surface was exposed. Thirty-three gauge syringe needles (Hamilton) were used to unilaterally infuse 0.3 μl of virus into the DR (bregma coordinates: anteroposterior, -4.36; mediolateral, 0; dorsoventral, -3.1) at a rate of 0.1 μl min⁻¹. Needles were removed 5 min after infusions were complete.

For optogenetic behavioural experiments, optic fibres (ferrules) were implanted above the DR (bregma coordinates: anteroposterior, -4.36; mediolateral, 0; dorsoventral, -3.0) for somatic stimulation or above the NAc bilaterally (bregma coordinates: anteroposterior, +1.5; mediolateral, ±0.75; dorsoventral, -3.9) or dorsal striatum bilaterally (bregma coordinates: anteroposterior, +0.5; mediolateral, ±1.6; dorsoventral, -2.7) for terminal stimulation. Ferrules were made in-house using 1.25 mm diameter multimode ceramic ferrules (ThorLab), 200 μm fibre optic cable with numerical aperture (NA) 0.39 (ThorLabSA) and blue dye epoxy (Fibre Instrument Sales). Ferrules were secured to the skull using miniature screws (thread size 00–90 × 1/16, Antrin Miniature Specialties) and light-cured dental adhesive cement (Geristore A&B paste, DenMat).

For drug infusions, a 26-gauge guide cannula, 3.6 mm in length from the cannula base, was implanted bilaterally into the NAc (bregma coordinates: anteroposterior, +1.5; mediolateral, ±0.75; dorsoventral, -3.9).

Optogenetic stimulation. For optogenetic photostimulation, ferrules were connected to a 473 nm laser diode (OEM Laser Systems) through a FC/PC adaptor and a fibre optic rotary joint (Doric Lenses). Laser output was controlled using a Master-8 pulse stimulator (A.M.P.I.), which delivered 5 ms light pulses at 20 Hz^{9,39,40,47,48}. Light output through the optical fibres was adjusted to ~5 mW (somatic) or ~15 mW (terminals) using a digital power meter console (ThorLabs). For activation of NpHR3.0, the optical fibre was connected to a 532 nm laser diode (Shanghai Dream Lasers Technology Co, Ltd) via a FC/PC adaptor and a fibre optic rotary joint (Doric Lenses). Laser output was again controlled using a Master-8 pulse stimulator (A.M.P.I.) and adjusted to ~10 mW. Mice received cycles of 8 s light on and 2 s light off.

Microinjection. One hour before behavioural experiments, mice received an intra-NAc infusion of 5-HT1b antagonist (NAS-181, 1.5 μg) or 5-HT1b agonist (CP93129, 0.5 μg) (Tocris Biosciences) or vehicle. Drugs were infused through an injector cannula using a microinfusion pump (Harvard Apparatus) at a continuous rate of 0.1 μl per min to a total volume of 0.3 μl per hemisphere. Injector cannulae were removed 2 min after infusions were complete, and mice were allowed to sit undisturbed for 1 h before behavioural tests.

Juvenile interaction assay. Juvenile interaction was performed in the home cage of the test animal as previously described¹⁷. Cagemates were temporarily moved to a holding container and the test mouse was habituated for 1 min. For optogenetic experiments, the fibre optic patch-cord was connected during the 1 min habituation period. After habituation, a novel conspecific juvenile mouse (3–5-week-old males) was placed into the home cage for 2 min of free interaction, with the laser on for the duration of the session during stimulation rounds. All sessions were video recorded with a camera located above the home cage and analysed manually following the behaviour. Interaction time was defined as those times during which the test mouse was actively exploring the juvenile mouse as defined by active

pursuit, sniffing any region (including the snout, body, and anogenital area) as well as grooming. These individual social behaviours were not assayed independently. Each test mouse underwent two rounds of the juvenile interaction assay, separated by 1 h, with a novel juvenile introduced during each session. Cohorts of mice were counterbalanced for the order of providing optogenetic stimulation versus no stimulation. All experiments and analyses were performed blinded without knowledge of the manipulation to which the subject had been subjected and the genotype of the subject.

Three-chamber sociability assay. A three-chamber sociability assay was performed in an arena with three separate chambers as previously described⁴⁹. On day one, the test mice were habituated to the arena, with two empty wire mesh cups placed in the two outer chambers for 5 min. Male, conspecific juvenile mice also habituated to the mesh cups for 5 min following test mice habituation. On day two, the test mouse was placed in the centre chamber and a conspecific juvenile (3–5-week-old males) was placed into one of the wire mesh cups. The tops of the mesh cups were covered so as to prevent mice from crawling on top. They were immobilized on the floor of the chambers and had mesh with square holes that were 0.8 × 0.8 cm. The test mice were placed in the centre chamber for 2 min. The barriers were then raised and the test mouse was allowed to explore freely for a 20 min session. For animals receiving optogenetic stimulation, mice had 5 min epochs of the laser being off or on, which were counterbalanced across mice. The placement of juvenile mice in the chamber was also counterbalanced across sessions. For the three-chamber assay using a high-fat food pellet, the pellet was placed under the wire mesh cup instead of a juvenile. Location of mice was assayed automatically using a video tracking system (BIOBSERVE). Sociability was calculated as: ((time in juvenile side - time in empty side)/(time in juvenile side + time in empty side)). These analyses are shown in Figs. 1–3 and 5. The actual times spent in each chamber during each 5 min epoch in all mouse cohorts are shown in Extended Data Figs. 1–11, which also illustrate the time spent within 3 cm of the mesh wire cups containing the juvenile (defined as proximity time).

Novel object interaction assay. The novel object interaction assay was performed in the exact same manner as the juvenile interaction assay, with either a toy mouse or a plastic block placed into the animal's home cage. The total time of investigation was again 2 min.

Open field test. To assay the effects of the different manipulations on locomotor activity, an open field test was conducted. Test mice were placed in an open field arena (40 × 40 cm) and allowed to move freely for an 18-min session. For animals receiving optogenetic stimulation, mice had 3 min epochs of laser being off or on, which were counterbalanced across mice. Time spent in the centre (25 × 25 cm) of the arena was also assayed as a measure of anxiety-related behaviour. Total distance travelled and centre time was assayed automatically using the video tracking system (BIOBSERVE) and compared between light on and light off epochs.

Real-time CPP. The real-time CPP protocol was conducted as described previously⁵⁰ in a rectangular Plexiglas cage with three chambers separated by removable Plexiglass walls. The left and right chambers each measured 28 × 24 cm and had distinct wall patterns (black and white stripes versus black and white squares) and flooring (smooth versus rough plastic floors). The centre chamber measured 11.5 × 24 cm with no wall patterns and a smooth clear floor. Subjects were placed in the centre compartment for 2 min at which point the barriers were lifted and the subject mouse was allowed to freely explore the entire apparatus for 15 min during which it was photostimulated (20 Hz, 5 ms pulses) whenever it entered the designated chamber, which was alternated between each testing session. Video tracking software (BIOBSERVE) recorded all animal movements and automatically analysed time spent and distance moved in each chamber. Preference was calculated by measuring total time in each chamber (stimulated, non-stimulated and centre).

Optical intracranial self-stimulation. Sixty-minute behavioural sessions were conducted in conditioning chambers (Med Associates Inc.) contained within sound-attenuating cubicles. Session start was indicated to the mouse by the illumination of a chamber light and the onset of low-volume white noise (65 dB) to mask external sounds. Two nosepoke ports, designated 'active' and 'inactive', were positioned on the left chamber wall. A response at the active nosepoke port resulted in optical stimulation (60 pulses, 5 ms duration, 20 Hz, 473 nm) on a fixed-ratio 1 schedule, with the exception that a new stimulation train could not be earned until any ongoing train had finished. Responses at the inactive nosepoke port were recorded but had no consequence. During the first training session, both nosepoke ports were baited with a crushed treat to facilitate initial investigation.

Fibre photometry. AAV-DJ-DIO-GCaMP6f was infused into the DR at the same stereotaxic coordinates noted previously, and a fibreoptic implant was advanced and secured at the same location. After allowing 3–4 weeks for viral expression, mice were first habituated to the fibre photometry apparatus for 30 min, and then tested on a subsequent day. Behaviour testing consisted of the juvenile interaction assay, as described above, with continuous video and fibre photometry acquisition. Fibre photometry data was acquired with Synapse software controlling an RZ5P lock-in amplifier (Tucker-Davis Technologies). GCaMP6f excitation was achieved

with a 473 nm LED (Doric), emission was measured with a femtowatt photoreceiver (2151; Newport), and signal was digitized as 6 kHz. All optical signals were band-pass filtered with a Fluorescence MiniCube FMC4 (Doric).

Signal processing was performed with Matlab (Mathworks, Inc.). In brief, signals were debleached by fitting with a mono- or bi-exponential decay function, and the resulting fluorescence trace was z-scored. Video was manually analysed by a genotype-blinded observer, who determined time of adult-to-juvenile contact. Peristimulus time histograms were constructed by taking the average of 7-s non-overlapping epochs of fluorescence consisting of 3 s before, and 4 s after contact time, which is defined as time = 0. Before averaging, each epoch was offset such that the z-score averaged from -3 to -1 s equalled 0. Peak z-scored fluorescence was determined for each peristimulus time histogram as the maximal z-score value between 0 and +4 s.

Electrophysiology. Mice were anaesthetized with isoflurane and coronal DR slices (250 μm) were prepared after intracardiac perfusions with ice-cold artificial cerebrospinal fluid (ACSF) which contained (in mM): 128 NaCl, 3 KCl, 1.25 NaH_2PO_4 , 10 D-glucose, 24 NaHCO_3 , 2 CaCl_2 and 2 MgCl_2 (oxygenated with 95% O_2 and 5% CO_2 , pH 7.4, 295–305 mOsm). Acute brain slices containing DR 5-HT neurons were generated using a microslicer (Leica VT1200S) in cold sucrose ACSF, which was derived by fully replacing NaCl with sucrose (254 mM) and saturated by 95% O_2 and 5% CO_2 . Slices were maintained in holding chambers with ACSF for 1 h at 32 °C. Patch pipettes (3–5 $\text{m}\Omega$) for whole-cell current-clamp and voltage-clamp recordings were pulled from borosilicate glass and filled with internal solution containing (in mM): 135 potassium gluconate, 10 HEPES, 4 KCl, 4 MgATP, and 0.3 NaGTP (pH 7.31, 287 mOsm).

Recordings from DR 5-HT neurons (identified visually by the presence of eYFP due to injection of DIO-eYFP into *Sert-cre* or *Sert-cre:16p11.2^{flx}* mice) were carried out in slices perfused with ACSF at 32 °C (flow rate = 2.5 ml min^{-1}). Recordings were made using a Multiclamp 700B amplifier. Signals were digitized at 8 kHz using an ITC-18 A/D converter (Instrutech Corporation) and filtered at 4 kHz. Data were acquired and analysed using Axograph-X (Axograph). For whole-cell recordings of spontaneous EPSCs, neurons were voltage clamped at -60 mV and series resistance (10–30 $\text{M}\Omega$) was monitored throughout the recordings with

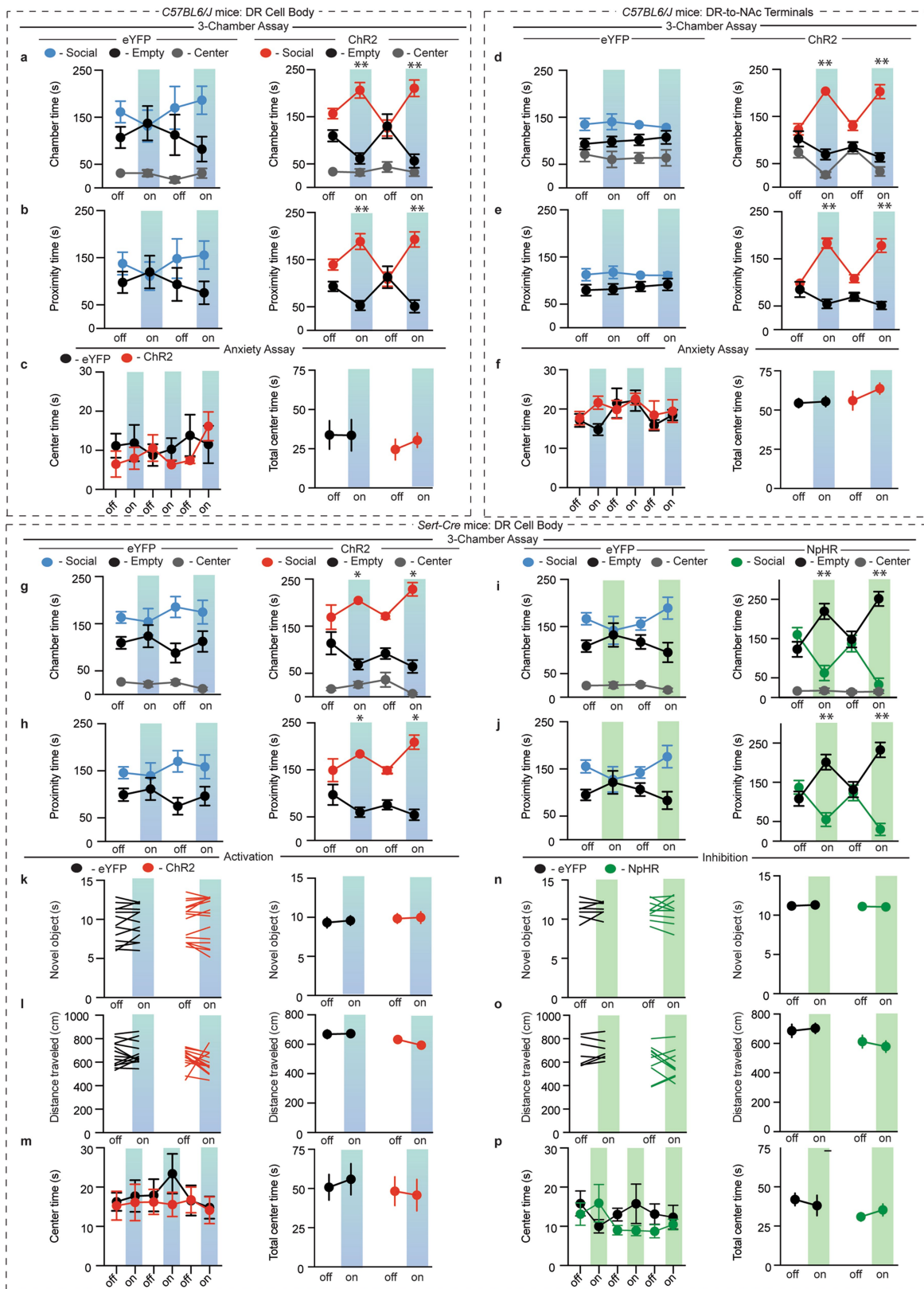
neurons discarded if resistance changed by >20%. At least 200 events per cell were acquired in 15 s blocks and detected using a threshold of 7 pA. Events were detected using Axograph event detection function and all events included in the final data analysis were verified by eye. To measure the intrinsic membrane properties of DR 5-HT neurons, whole-cell recordings were carried out in current-clamp mode at -60 mV and spikes were induced by incremental increases of current injection (each step increase was 50 pA; range 50–200 pA). Spike numbers were counted by eye. All data acquisition and analyses were performed blinded to the genotype of the cells from which recordings were made.

Blinding and statistics. As mentioned above, for all data acquisition and analyses in this study, investigators were blinded to the manipulation that the experimental subject had received and the genotype of the subject. Student's *t*-tests were used to compare two groups. Kolmogorov–Smirnov test was used for cumulative probability plots. One-way ANOVA with Tukey's post hoc test was used to compare multiple groups. Two-way ANOVA was used for analysis of multiple groups with Sidak's or Tukey's multiple comparison post hoc test, when appropriate. Statistical analyses were performed using Prism 6.0 (GraphPad Software). All data were tested and shown to exhibit normality and equal variances. All data are expressed as mean \pm s.e.m.

Reporting summary. Further information on experimental design is available in the Nature Research Reporting Summary linked to this paper.

Data availability. All data are available from the corresponding author upon reasonable request.

47. Sharp, T., Bramwell, S. R., Clark, D. & Grahame-Smith, D. G. *In vivo* measurement of extracellular 5-hydroxytryptamine in hippocampus of the anaesthetized rat using microdialysis: changes in relation to 5-hydroxytryptaminergic neuronal activity. *J. Neurochem.* **53**, 234–240 (1989).
48. Hayashi, K., Nakao, K. & Nakamura, K. Appetitive and aversive information coding in the primate dorsal raphe nucleus. *J. Neurosci.* **35**, 6195–6208 (2015).
49. Kaidanovich-Bellin, O., Lipina, T., Vukobradovic, I., Roder, J. & Woodgett, J. R. Assessment of social interaction behaviors. *J. Vis. Exp.* **48**, 2473 (2011).
50. Lammel, S. et al. Input-specific control of reward and aversion in the ventral tegmental area. *Nature* **491**, 212–217 (2012).



Extended Data Fig. 1 | See next page for caption.

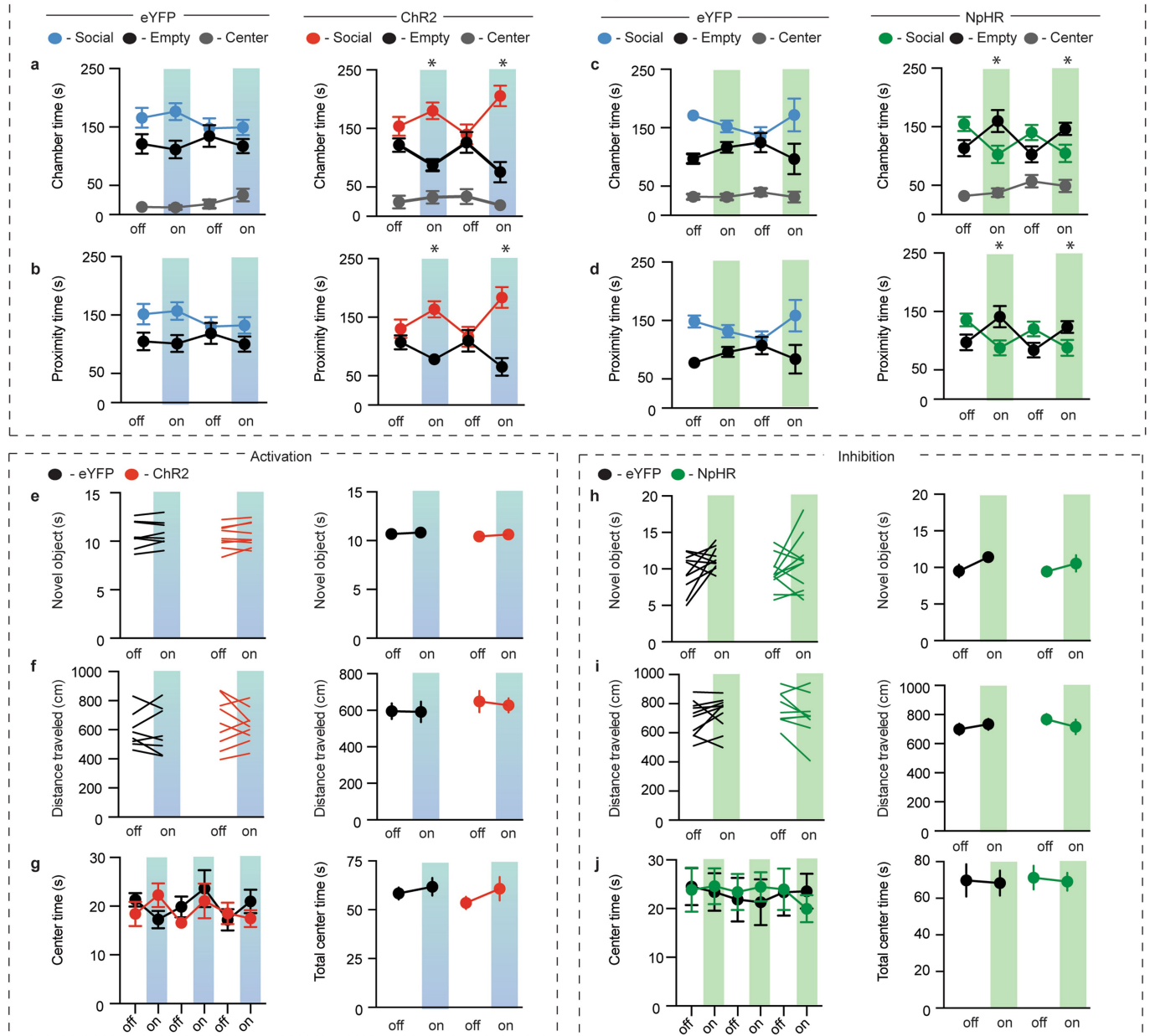
Extended Data Fig. 1 | Activation of DR neurons or their NAc projections increases sociability, and bidirectional modulation of DR 5-HT neuron activity bidirectionally modifies sociability.

a, b, Quantification of chamber time (**a**: eYFP, $F_{6,45} = 0.6823$, $P = 0.6647$, $n = 6$; ChR2, $F_{6,72} = 17.21$, $P < 0.01$, $n = 9$) and proximity time (**b**: eYFP, $F_{3,30} = 0.7517$, $P = 0.5300$, $n = 6$; ChR2, $F_{3,48} = 32.96$, $P < 0.01$, $n = 9$) in the three-chamber assay. **c**, Quantification of centre time in the locomotion assay (**c**: $F_{5,65} = 1.263$, $P = 0.2908$, $n = 6-9$). **d, e**, Quantification of chamber time (**d**: eYFP, $F_{6,54} = 0.2602$, $P = 0.9529$, $n = 7$; ChR2, $F_{6,72} = 19.36$, $P < 0.01$, $n = 9$) and proximity time (**e**: eYFP, $F_{3,36} = 0.3456$, $P = 0.7925$, $n = 7$; ChR2, $F_{3,48} = 26.44$, $P < 0.01$, $n = 9$) in the three-chamber assay. **f**, Quantification of centre time in the locomotion assay ($F_{5,40} = 0.7786$, $P = 0.5710$, $n = 5$). **g, h**, Quantification of chamber time (**g**: eYFP, $F_{6,54} = 0.7293$, $P = 0.6280$, $n = 7$; ChR2, $F_{6,72} = 3.812$, $P < 0.05$, $n = 9$) and proximity time (**h**: eYFP, $F_{3,36} = 0.9256$, $P = 0.4383$, $n = 7$; ChR2, $F_{3,48} = 4.844$, $P < 0.05$, $n = 9$) in the three-

chamber assay. **i, j**, Quantification of chamber time (**i**: eYFP, $F_{6,54} = 1.058$, $P = 0.3989$, $n = 7$; NpHR, $F_{6,81} = 13.04$, $P < 0.01$, $n = 10$) and proximity time (**j**: eYFP, $F_{3,36} = 1.661$, $P = 0.1926$, $n = 7$; NpHR, $F_{3,54} = 16.29$, $P < 0.01$, $n = 10$) in the three-chamber assay. **k, l**, Quantification of novel object interaction assay (**k**: $F_{1,52} = 0.01018$, $P = 0.9200$, $n = 13-15$), locomotion assay (**l**: $F_{1,52} = 0.7626$, $P = 0.3865$, $n = 13-15$), and centre time (**m**: $F_{5,130} = 0.766$, $P = 0.5759$, $n = 13-15$) in *Sert-cre* mice expressing DIO-eYFP or DIO-ChR2 in DR receiving soma stimulation. **n-p**, Quantification of novel object interaction assay (**n**: $F_{1,30} = 0.04112$, $P = 0.8407$, $n = 7-10$), locomotion assay (**o**: $F_{1,30} = 0.3837$, $P = 0.5403$, $n = 7-10$), and centre time (**p**: $F_{5,80} = 1.195$, $P = 0.3190$, $n = 8-10$) in *Sert-cre* mice expressing DIO-eYFP or DIO-NpHR in DR receiving soma stimulation. Data are mean \pm s.e.m. * $P < 0.05$, ** $P < 0.01$, two-way ANOVA with Tukey's multiple comparison post hoc test. Comparisons with no asterisk had $P > 0.05$ and were considered not significant.

Sert-Cre mice: DR-to-NAc Terminals

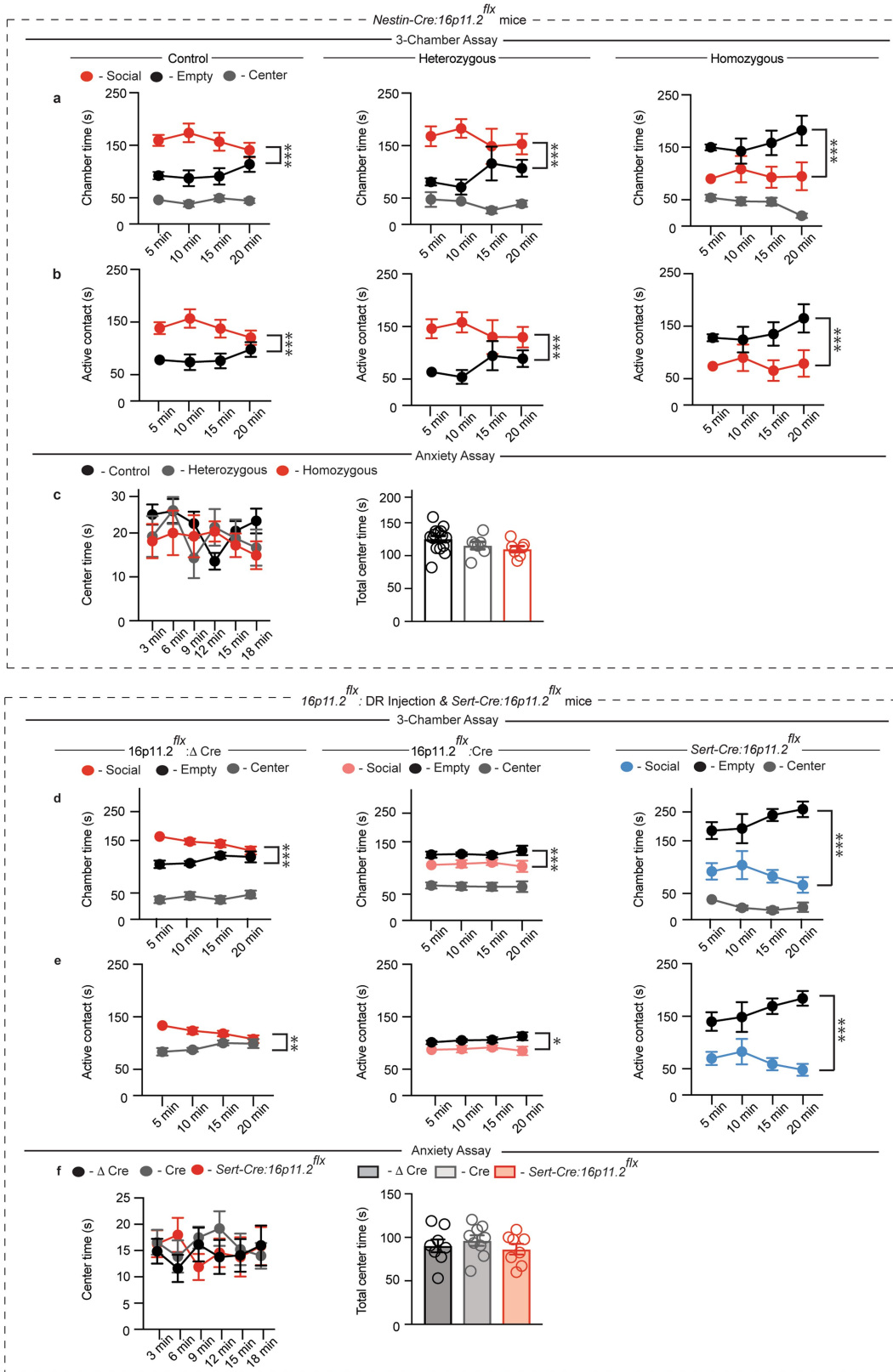
3-Chamber Assay



Extended Data Fig. 2 | Bidirectional modulation of DR-to-NAc 5-HT terminals modifies sociability, but not control behaviours.

a, b, Quantification of chamber time (**a**: eYFP, $F_{6,63} = 1.383$, $P = 0.2352$, $n = 8$; ChR2, $F_{6,72} = 4.891$, $P < 0.05$, $n = 9$) and proximity time (**b**: eYFP, $F_{3,42} = 0.9652$, $P = 0.4181$, $n = 8$; ChR2, $F_{3,48} = 7.565$, $P < 0.05$, $n = 9$) in the three-chamber assay. **c, d**, Quantification of chamber time (**c**: eYFP, $F_{6,81} = 1.626$, $P = 0.1506$, $n = 10$; NpHR, $F_{6,81} = 6.253$, $P < 0.05$, $n = 10$) and proximity time (**d**: eYFP, $F_{3,54} = 2.304$, $P = 0.0872$, $n = 10$; NpHR, $F_{3,54} = 7.821$, $P < 0.05$, $n = 10$) in the three-chamber assay. **e–g**, Quantification of novel object interaction assay (**e**: $F_{1,30} = 0.00206$, $P = 0.9641$, $n = 8–9$), locomotion assay (**f**: $F_{1,30} = 0.03023$, $P = 0.8631$,

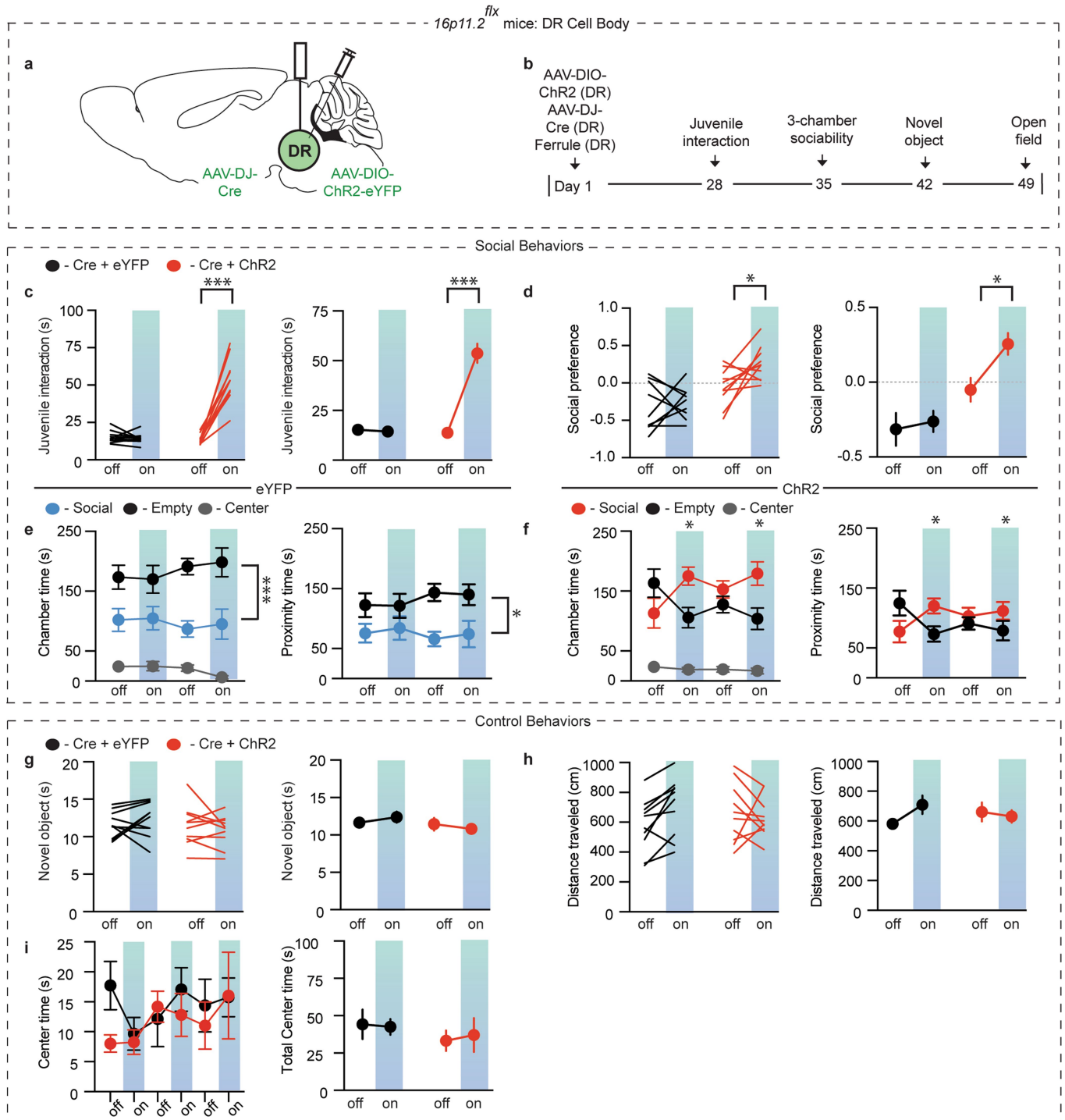
$n = 8–9$), and centre time (**g**: $F_{5,75} = 1.205$, $P = 0.3151$, $n = 8–9$) in *Sert-cre* mice expressing DIO-eYFP or DIO-ChR2 in DR receiving DR-to-NAc terminal stimulation. **h–j**, Quantification of novel object interaction assay (**h**: $F_{1,38} = 0.213$, $P = 0.6471$, $n = 10–11$), locomotion assay (**i**: $F_{1,34} = 1.077$, $P = 0.3066$, $n = 9–10$), and centre time (**j**: $F_{5,90} = 0.1646$, $P = 0.9749$, $n = 9–10$) in *Sert-cre* mice expressing DIO-eYFP or DIO-NpHR in DR receiving DR-to-NAc terminal stimulation. Data are mean \pm s.e.m. * $P < 0.05$, ** $P < 0.01$; repeated measures, two-way ANOVA with Tukey's multiple comparison post hoc test. Comparisons with no asterisk had $P > 0.05$ and were considered not significant.



Extended Data Fig. 3 | See next page for caption.

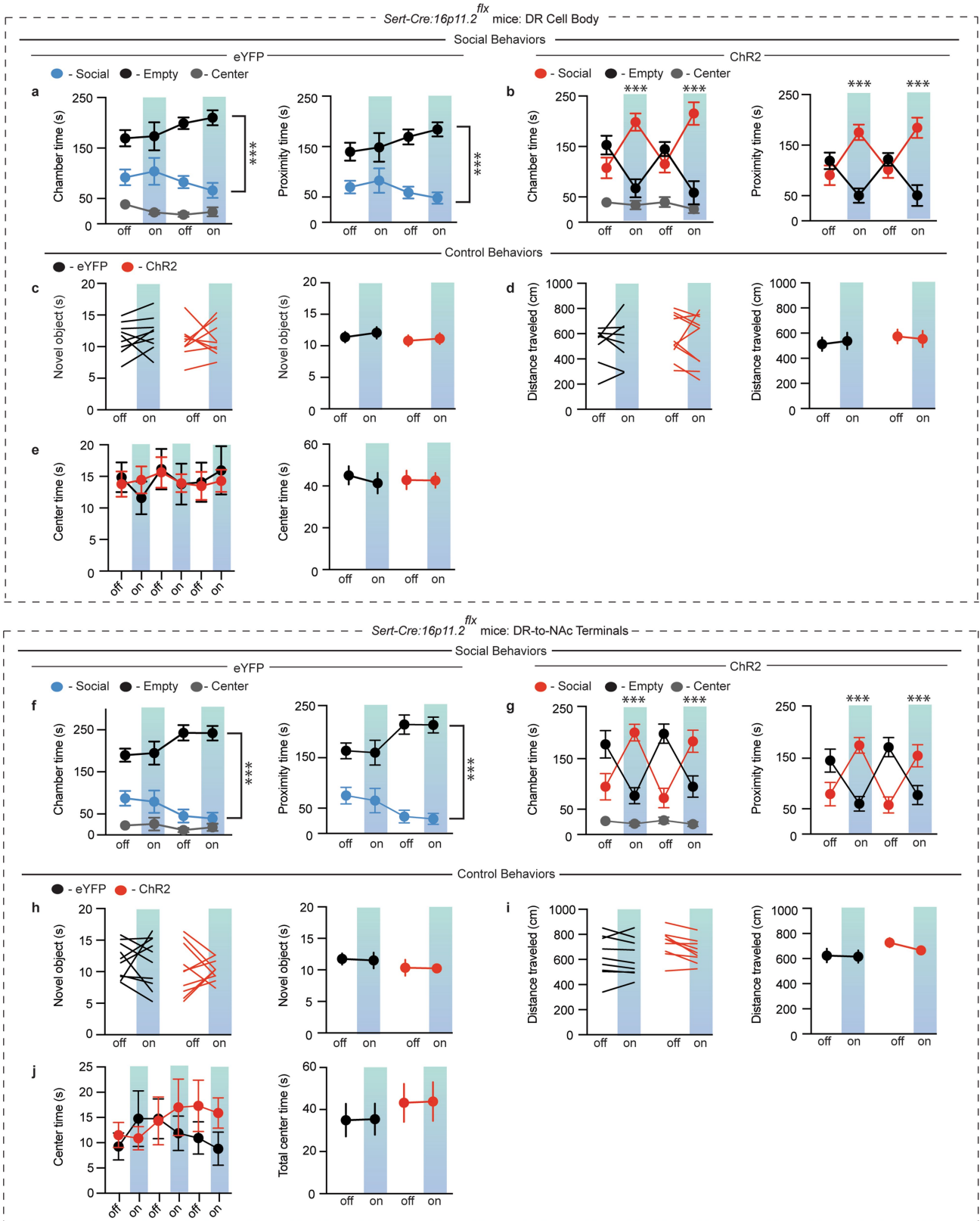
Extended Data Fig. 3 | 16p11.2 deletion decreases sociability, but not an anxiety-related behaviour. a, b, Quantification of chamber time (a: control, $F_{2,45} = 39.5$, $P < 0.001$, $n = 16$; heterozygous, $F_{2,21} = 23.39$, $P < 0.001$, $n = 8$; homozygous, $F_{2,21} = 31.54$, $P < 0.001$, $n = 8$) and proximity time (b: control, $F_{1,30} = 14.61$, $P < 0.001$, $n = 16$; heterozygous, $F_{1,14} = 10.14$, $P < 0.01$, $n = 8$; homozygous, $F_{1,14} = 11.88$, $P < 0.01$, $n = 8$) in the three-chamber assay. **c,** Quantification of centre time (c: $F_{10,135} = 1.03$, $P = 0.4215$, $n = 7-15$) in control, heterozygous $16p11.2^{flx}:Nes-creER$ and homozygous $16p11.2^{flx}:Nes-creER$ mice. **d, e,** Quantification of chamber time in the three-chamber assay (d: $16p11.2^{flx}:\Delta cre$, $F_{2,24} = 121.2$,

$P < 0.001$, $n = 9$; $16p11.2^{flx}:cre$, $F_{2,24} = 27.86$, $P < 0.001$, $n = 9$; $Sert-cre:16p11.2^{flx}$, $F_{2,21} = 84.95$, $P < 0.001$, $n = 8$) and proximity time (e: $16p11.2^{flx}:\Delta cre$, $F_{1,16} = 26.13$, $P < 0.001$, $n = 9$; $16p11.2^{flx}:cre$, $F_{1,16} = 6.885$, $P < 0.05$, $n = 9$; $Sert-cre:16p11.2^{flx}$, $F_{1,14} = 44.00$, $P < 0.001$, $n = 8$). **f,** Quantification of centre time in (c: $F_{2,22} = 0.6019$, $P = 0.5565$, $n = 8-9$) $16p11.2^{flx}:\Delta cre$, $16p11.2^{flx}:cre$ and $Sert-cre:16p11.2^{flx}$ mice. Data are mean \pm s.e.m. * $P < 0.05$, ** $P < 0.01$, *** $P < 0.001$; repeated measures, two-way ANOVA with Tukey's multiple comparison post hoc test. Comparisons with no asterisk had $P > 0.05$ and were considered not significant.



Extended Data Fig. 4 | Optogenetic activation of DR neurons reverses social deficits induced by $16p11.2$ deletion, but does not alter control behaviours. **a**, Schematic of AAV-DJ-Cre and DIO-ChR2 injected into and optic fibre implanted above the DR in $16p11.2^{flx}$ mice. **b**, Timeline of behavioural experiments. **c**, **d**, Quantification of sociability during juvenile interaction (**c**: $F_{1,36} = 62.43$, $P < 0.001$, $n = 10$) and the three-chamber sociability assay (**d**: $F_{1,34} = 2.298$, $P < 0.05$, $n = 9-10$) in $16p11.2^{flx}$ mice expressing DIO-eYFP or DIO-ChR2 and AAV-DJ-Cre in DR receiving soma stimulation. **e**, **f**, Quantification of chamber and proximity time in the three-chamber assay (**e**: eYFP, $F_{2,24} = 92.48$, $P < 0.001$, $n = 9$ (left);

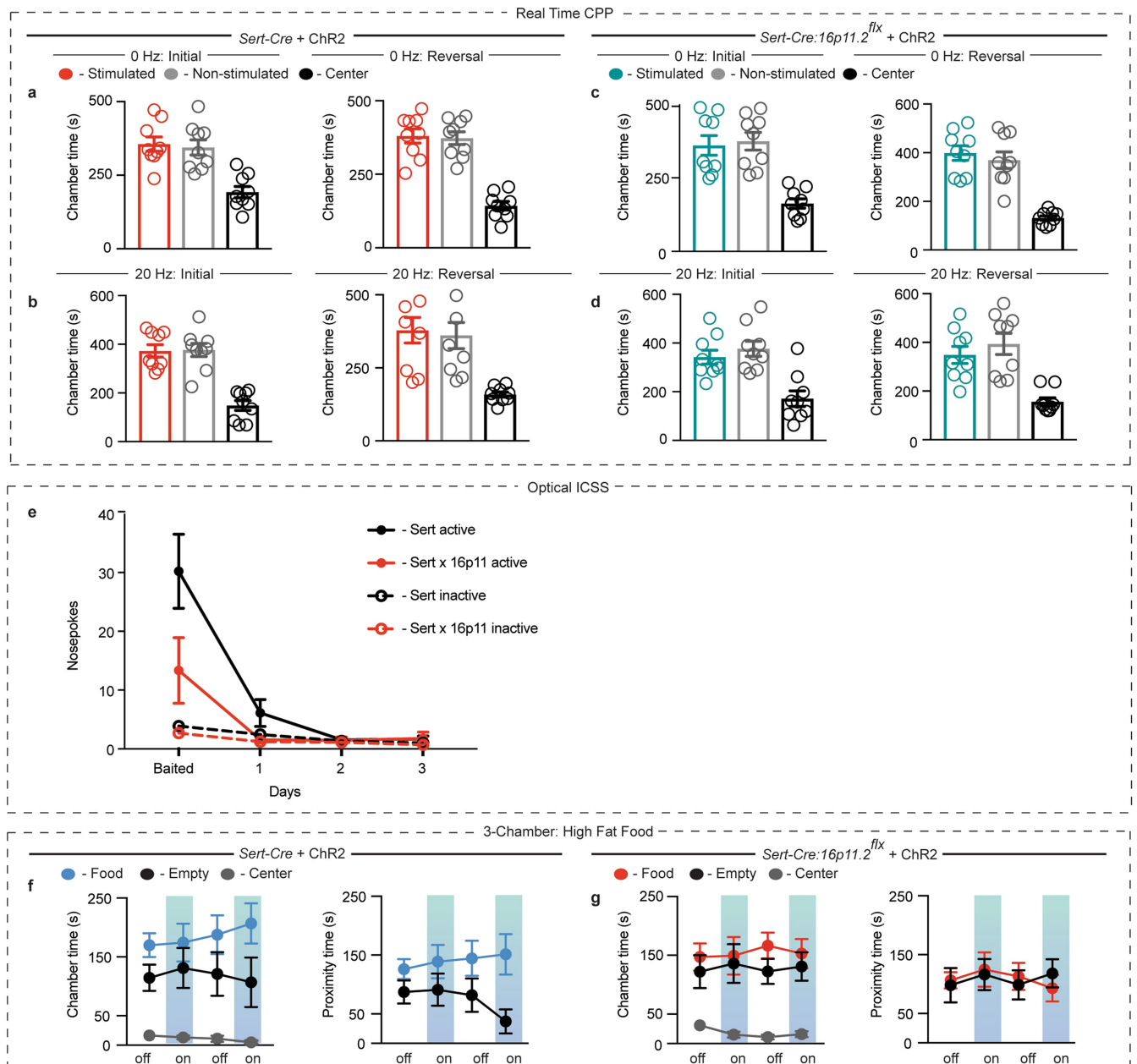
$F_{1,16} = 17.53$, $P < 0.05$, $n = 9$ (right); **f**: ChR2, $F_{6,81} = 3.085$, $P < 0.05$, $n = 10$ (left); $F_{3,54} = 3.493$, $P < 0.05$, $n = 10$ (right)). **g-i**, Quantification of novel object interaction assay (**g**: $F_{1,36} = 0.956$, $P = 0.3424$, $n = 10$), locomotion assay (**h**: $F_{1,36} = 1.962$, $P = 0.1698$, $n = 10$), and centre time (**i**: $F_{5,90} = 0.7668$, $P = 0.5761$, $n = 10$) in $16p11.2^{flx}$ mice. Data are mean \pm s.e.m. * $P < 0.05$, *** $P < 0.001$; repeated measures, two-way ANOVA with Tukey's multiple comparison post hoc test. Comparisons with no asterisk had $P > 0.05$ and were considered not significant. The schematic of the mouse brain in this figure has been adapted with permission from Franklin & Paxinos⁴⁶.



Extended Data Fig. 5 | See next page for caption.

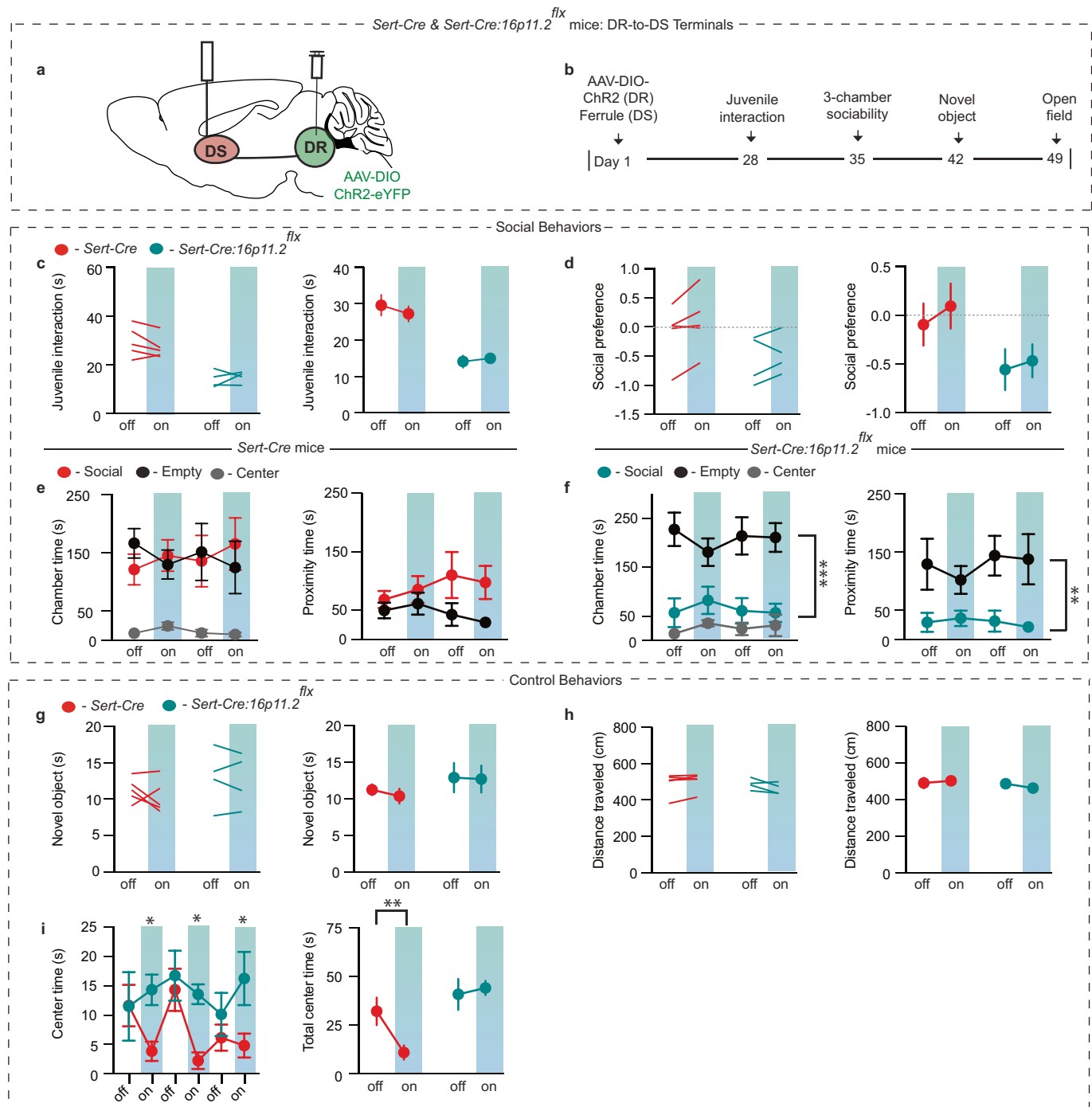
Extended Data Fig. 5 | Optogenetic activation of DR 5-HT neurons or DR-to-NAc 5-HT terminals rescues social deficits induced by 16p11.2 deletion, but does not alter control behaviours. **a, b**, Quantification of chamber and proximity time in the three-chamber assay (**a**: eYFP, $F_{2,21} = 84.95$, $P < 0.001$, $n = 8$ (left); $F_{1,14} = 44.00$, $P < 0.001$, $n = 8$ (right); **b**: ChR2, $F_{6,81} = 9.26$, $P < 0.001$, $n = 10$ (left); $F_{3,54} = 11.54$, $P < 0.001$, $n = 10$ (right)). **c–e**, Quantification of the novel object interaction assay (**c**: $F_{1,32} = 0.03819$, $P = 0.8463$, $n = 9$), locomotion assay (**d**: $F_{1,32} = 0.141$, $P = 0.7097$, $n = 8–10$), and centre time (**e**: $F_{5,80} = 0.195$, $P = 0.9636$, $n = 8–10$) in *Sert-cre:16p11.2^{flx}* mice expressing DIO-eYFP or DIO-ChR2 in DR receiving soma stimulation. **f, g**, Quantification of chamber

and proximity time in the three-chamber assay (**f**: eYFP, $F_{2,27} = 73.89$, $P < 0.001$, $n = 10$ (left); $F_{1,18} = 63.38$, $P < 0.001$, $n = 10$ (right); **g**: ChR2, $F_{6,81} = 11.33$, $P < 0.001$, $n = 10$ (left); $F_{3,54} = 14.55$, $P < 0.001$, $n = 10$ (right)). **h–j**, Quantification of novel object interaction assay (**h**: $F_{1,36} = 0.01038$, $P = 0.9194$, $n = 10$), locomotion assay (**i**: $F_{1,32} = 0.3655$, $P = 0.5497$, $n = 9$), and centre time (**j**: $F_{5,90} = 0.9092$, $P = 0.4788$, $n = 10$) in *Sert-cre:16p11.2^{flx}* mice expressing DIO-eYFP or DIO-ChR2 in DR receiving DR-to-NAc 5-HT terminal stimulation. Data are mean \pm s.e.m. *** $P < 0.001$; repeated measures, two-way ANOVA with Tukey's multiple comparison post hoc test. Comparisons with no asterisk had $P > 0.05$ and were considered not significant.



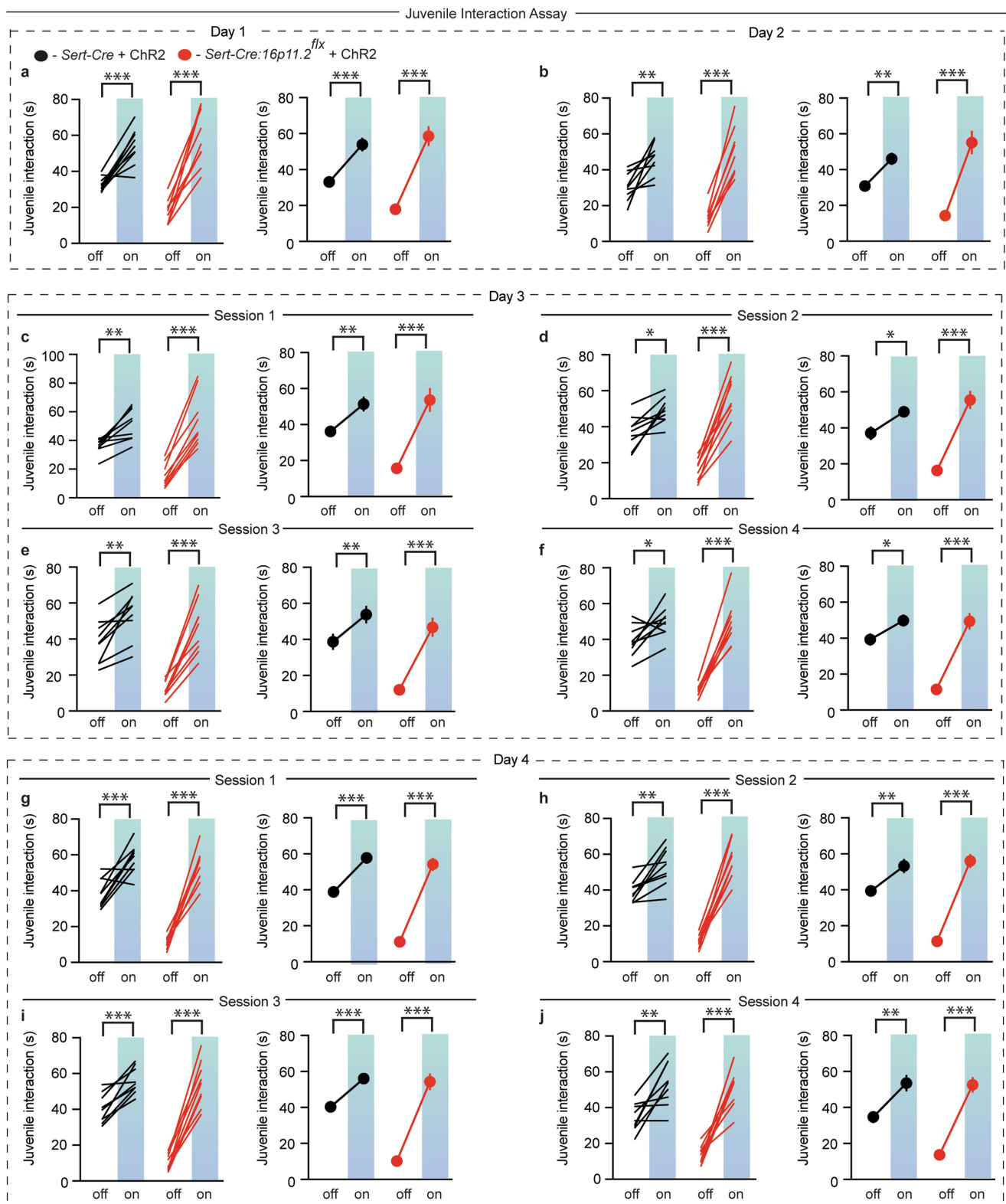
Extended Data Fig. 6 | 5-HT release in the NAc is not acutely reinforcing. **a, b**, Quantification of chamber time in the real-time CPP assay for 0 Hz (**a**) and 20 Hz (**b**) stimulation for initial (left) and reversal (right) stimulations (**a**: 0 Hz initial $F_{2,16} = 10.22$, $P < 0.05$, $n = 9$; 0 Hz reversal $F_{2,16} = 29.01$, $P < 0.001$, $n = 9$; **b**: 20 Hz initial $F_{2,16} = 19.37$, $P < 0.001$, $n = 9$; 20 Hz reversal $F_{2,16} = 7.53$, $P < 0.01$, $n = 9$) in *Sert-cre* mice receiving DR-to-NAc terminal stimulation. **c, d**, Quantification of chamber time in the real-time CPP assay for 0 Hz (**c**) and 20 Hz (**d**) stimulation for initial (left) and reversal (right) stimulations (**c**: 0 Hz initial $F_{2,16} = 12.44$, $P < 0.001$, $n = 9$; 0 Hz reversal $F_{2,16} = 19.92$, $P < 0.001$, $n = 9$; **d**: 20 Hz initial $F_{2,16} = 8.56$, $P < 0.01$, $n = 9$; 20 Hz reversal $F_{2,16} = 9.517$, $P < 0.001$, $n = 9$) in *Sert-cre:16p11.2^{flx}* mice receiving DR-to-NAc terminal stimulation. **e**, Quantification of nosepokes for active and inactive

ports for *Sert-cre* and *Sert-cre:16p11.2^{flx}* mice (*Sert-cre* $F_{2,32} = 1.9$, $P = 0.1655$, $n = 9$; *Sert-cre:16p11.2^{flx}* $F_{2,32} = 0.25$, $P = 0.7821$, $n = 9$). **f, g**, Quantification of chamber time (left) and proximity time (right) in high-fat food three-chamber assay for *Sert-cre* mice ($F_{6,72} = 0.6713$, $P = 0.6731$, $n = 9$; $F_{3,48} = 1.495$, $P = 0.2279$, $n = 10$) and *Sert-cre:16p11.2^{flx}* mice ($F_{6,72} = 0.4006$, $P = 0.8763$, $n = 10$; $F_{3,48} = 0.4157$, $P = 0.7425$, $n = 10$) (**g**). Post-hoc analysis showed no significant difference between stimulated and non-stimulated chambers. * $P < 0.05$, ** $P < 0.01$, *** $P < 0.001$; repeated measures, one-way (**a-d**) or two-way (**f, g**) ANOVA with Tukey's multiple comparison post hoc test, or one-way ANOVA with Sidak's multiple comparison post hoc test comparing active to inactive nosepokes (**e**). Comparisons with no asterisk had $P > 0.05$ and were considered not significant.



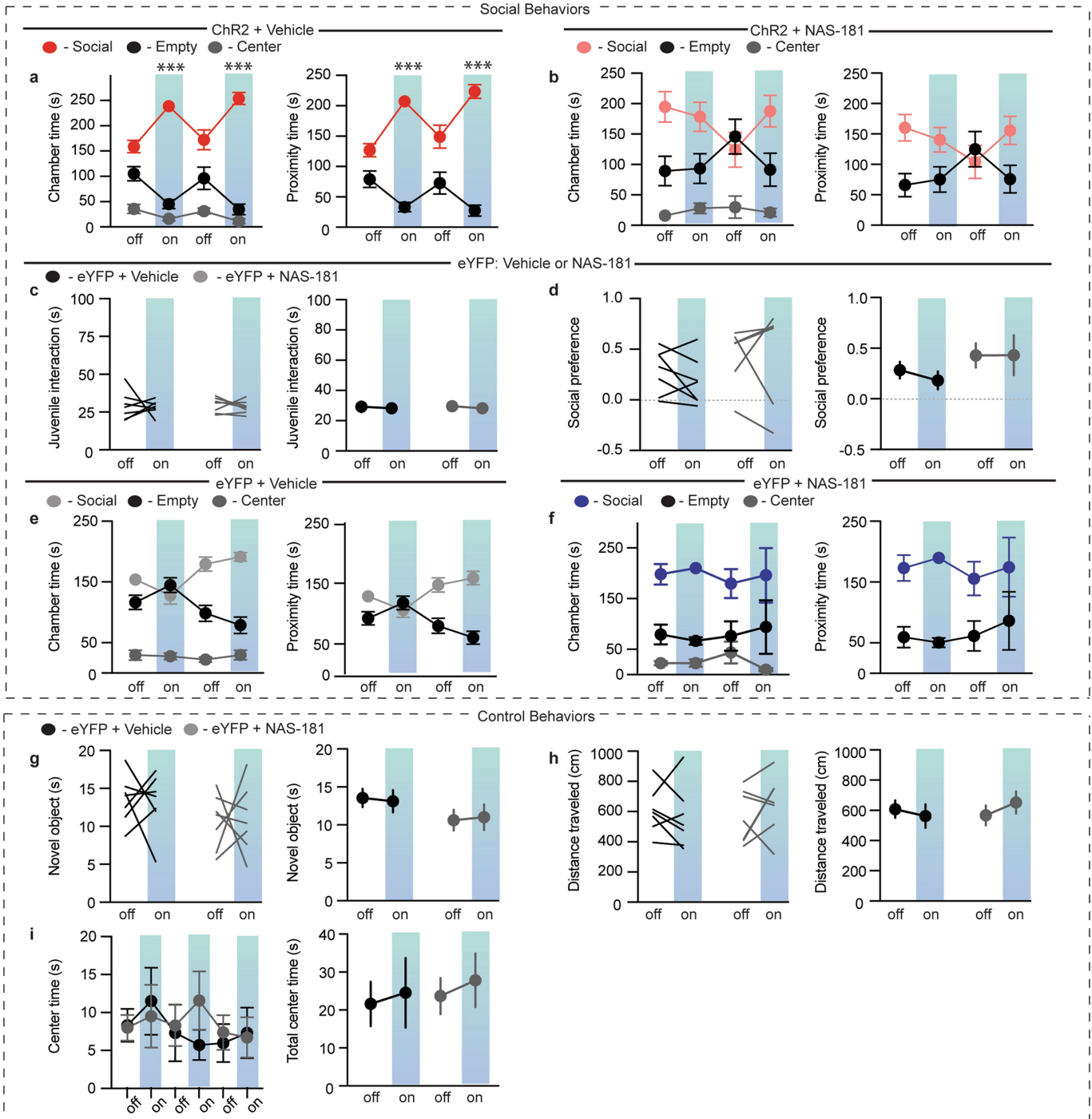
Extended Data Fig. 7 | Activation of DR 5-HT terminals in the dorsal striatum does not enhance sociability nor rescue social deficits induced by 16p11.2 deletion. **a**, Schematic of DIO-ChR2-eYFP injected into the DR and optic fibre implanted above the dorsal striatum (DS) in *Sert-cre* or *Sert-cre:16p11.2^{flx}* mice. **b**, Timeline of behavioural experiments. **c**, **d**, Quantification of sociability during the juvenile interaction assay (c: $F_{1,14} = 0.5429$, $P = 0.4734$, $n = 4-5$) and sociability in the three-chamber assay (d: $F_{1,14} = 0.055$, $P = 0.8177$, $n = 4-5$) in *Sert-cre* or *Sert-cre:16p11.2^{flx}* mice expressing DIO-eYFP or DIO-ChR2 with terminal stimulation of DR 5-HT neurons in the dorsal striatum. **e**, **f**, Quantification of the three-chamber assay showing chamber (left) and proximity (right)

time (e: *Sert-cre*, $F_{6,36} = 1.078$, $P = 0.3939$, $n = 5$ (left); $F_{3,24} = 2.009$, $P = 0.1395$, $n = 5$ (right); *Sert-cre:16p11.2^{flx}*, $F_{2,9} = 16.44$, $P < 0.001$, $n = 4$ (left); $F_{1,6} = 11.2$, $P < 0.01$, $n = 4$ (right)). **g-i**, Quantification of novel object interaction assay (**g**: $F_{1,14} = 0.058$, $P = 0.8125$, $n = 4-5$), locomotion assay (**h**: $F_{1,14} = 0.6195$, $P = 0.4444$, $n = 4-5$), and centre time (**i**: $F_{1,7} = 8.292$, $P < 0.05$, $n = 4-5$) in *Sert-cre* or *Sert-cre:16p11.2^{flx}* mice. Data are mean \pm s.e.m. * $P < 0.05$, ** $P < 0.01$, *** $P < 0.001$; repeated measures, two-way ANOVA with Tukey's multiple comparison post hoc test. Comparisons with no asterisk had $P > 0.05$ and considered were not significant. The schematic of the mouse brain in this figure has been adapted with permission from Franklin & Paxinos⁴⁶.



Extended Data Fig. 8 | Activation of DR-to-NAc 5-HT terminals does not elicit long-lasting effects on sociability. a–j, Quantification of sociability during juvenile interaction assay on day 1 of stimulation (a: $F_{1,16} = 10.65$, $P < 0.001$, $n = 9$), day 2 (b: $F_{1,16} = 16.71$, $P < 0.01$, $n = 9$), day 3 session 1 (c: $F_{1,16} = 17.7$, $P < 0.01$, $n = 9$), session 2 (d: $F_{1,16} = 27.05$, $P < 0.05$, $n = 9$), session 3 (e: $F_{1,16} = 13.35$, $P < 0.01$, $n = 9$), session 4 (f: $F_{1,16} = 25.03$, $P < 0.05$, $n = 9$) and day 4 session 1 (g: $F_{1,16} = 17.41$,

$P < 0.001$, $n = 9$), session 2 (h: $F_{1,16} = 39.76$, $P < 0.01$, $n = 9$), session 3 (i: $F_{1,16} = 35.49$, $P < 0.001$, $n = 9$), and session 4 (j: $F_{1,16} = 8.295$, $P < 0.01$, $n = 9$) in Sert-cre or Sert-cre:16p11.2^{flx} mice expressing DIO-ChR2 with DR-to-NAc 5-HT terminal stimulation. Data are mean \pm s.e.m. * $P < 0.05$, ** $P < 0.01$, *** $P < 0.001$; repeated measures, two-way ANOVA with Tukey's multiple comparison post hoc test.

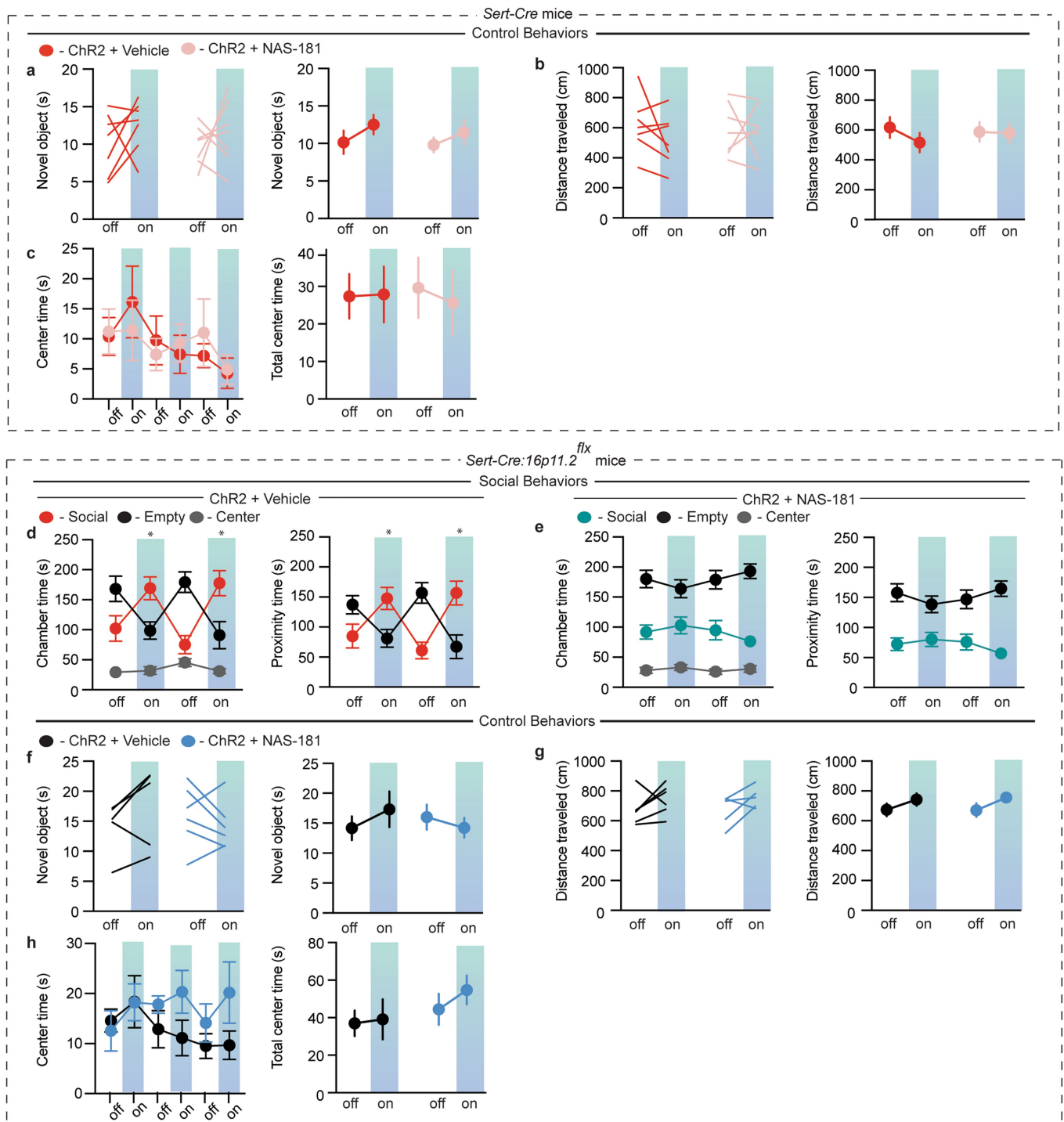


Extended Data Fig. 9 | 5-HT_{1b} receptor antagonist infusion into NAc blocks enhanced sociability due to DR 5-HT neuron stimulation.

a, Quantification of chamber and proximity time in the three-chamber assay (**a**: ChR2 + vehicle, $F_{6,54} = 15.15$, $P < 0.001$, $n = 7$ (left); $F_{3,36} = 18.00$, $P < 0.001$, $n = 7$ (right); **b**: ChR2 + NAS-181, $F_{6,45} = 1.479$, $P = 0.2069$, $n = 6$ (left); $F_{3,30} = 1.926$, $P = 0.1467$, $n = 6$ (right)) in *Sert-cre* mice expressing DIO-ChR2 in DR with either vehicle (red) or NAS-181 (pink) infused into the NAc before analysis of behaviour. **c**, **d**, Quantification of sociability during the juvenile interaction assay (**c**: $F_{1,24} = 0.004638$, $P = 0.9463$, $n = 7$) and the three-chamber assay (**d**: $F_{1,22} = 0.1686$, $P = 0.1686$, $n = 6-7$) in *Sert-cre* mice expressing DIO-eYFP in DR with either vehicle (black) or NAS-181 (grey) infused into NAc before behaviour. **e**, **f**, Quantification of the three-chamber assay showing

chamber and proximity time (**e**: eYFP + vehicle, $F_{6,54} = 12.36$, $P < 0.001$, $n = 7$ (left); $F_{3,36} = 15.98$, $P < 0.01$, $n = 7$ (right); **f**: eYFP + NAS-181, $F_{6,45} = 0.4512$, $P = 0.8403$, $n = 6$ (left); $F_{3,30} = 0.7365$, $P = 0.7365$, $n = 6$ (right)) in *Sert-cre* mice expressing DIO-eYFP in DR with either vehicle (grey) or NAS-181 (blue) infused into the NAc before analysis of behaviour. **g-i**, Quantification of the novel object interaction assay (**g**: $F_{1,24} = 0.0791$, $P = 0.7809$, $n = 7$), locomotion assay (**h**: $F_{1,24} = 0.8954$, $P = 0.3535$, $n = 7$), and centre time (**i**: $F_{5,60} = 0.6042$, $P = 0.6969$, $n = 7$) in *Sert-cre* mice expressing DIO-eYFP in DR with either vehicle (grey) or NAS-181 (blue) infused into the NAc before behaviour. Data are mean \pm s.e.m. *** $P < 0.001$; repeated measures, two-way ANOVA with Tukey's multiple comparison post hoc test. Comparisons with no asterisk had $P > 0.05$ and were considered not significant.

5-HT1b Antagonist: NAc Infusion

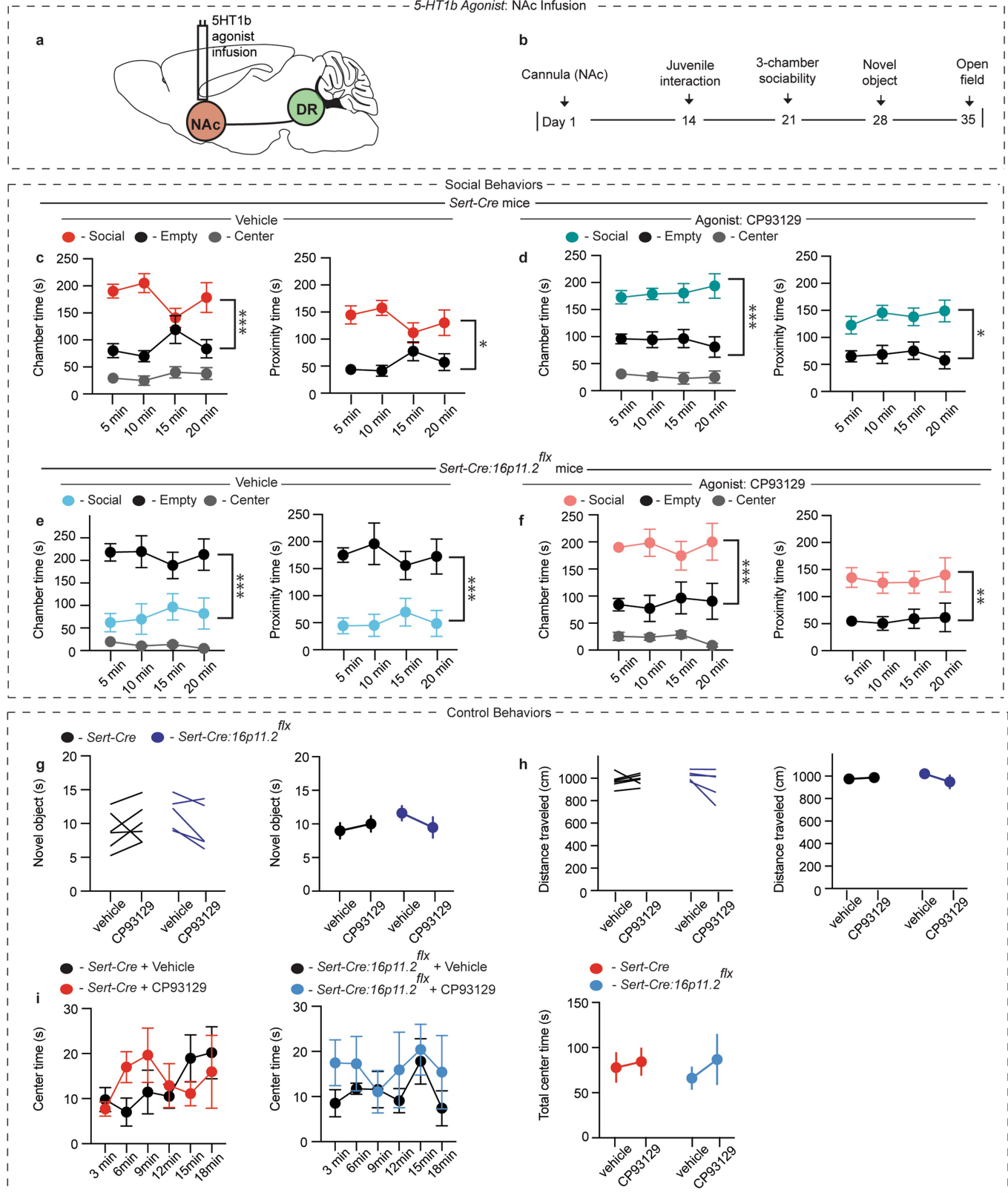


Extended Data Fig. 10 | 5-HT1b receptor antagonist infusion into the NAc does not alter control behaviours and blocks rescue of 16p11.2 deletion social deficits by DR 5-HT neuron stimulation.

a–c, Quantification of the novel object interaction assay (**a**: $F_{1,24} = 0.0579$, $P = 0.8120$, $n = 7$), locomotion assay (**b**: $F_{1,24} = 0.4764$, $P = 0.4967$, $n = 7$), and centre time (**c**: $F_{5,60} = 0.3936$, $P = 0.8513$, $n = 7$) in *Sert-cre* mice expressing DIO-ChR2 in DR with either vehicle (red) or NAS-181 (pink) infused into the NAc before behaviour. **d, e**, Quantification of chamber and proximity time in the three-chamber assay (**d**: ChR2 + vehicle, $F_{6,90} = 9.03$, $P < 0.05$, $n = 11$ (left); $F_{3,60} = 13.04$, $P < 0.05$, $n = 11$ (right); **e**: ChR2 + NAS-181, $F_{6,90} = 1.226$, $P = 0.3004$, $n = 11$ (left); $F_{3,60} = 1.69$,

$P = 0.1786$, $n = 11$ (right)) in *Sert-cre:16p11.2^{flx}* mice expressing DIO-ChR2 in DR with either vehicle (red) or NAS-181 (aqua) infused into the NAc before behaviour assays during optogenetic stimulation. **f–h**, Quantification of novel object interaction assay (**f**: $F_{1,18} = 0.1263$, $P = 0.2758$, $n = 5–6$), locomotion assay (**g**: $F_{1,18} = 0.0344$, $P = 0.8549$, $n = 5–6$), and centre time (**h**: $F_{5,45} = 1.22$, $P = 0.3155$, $n = 5–6$) in *Sert-cre:16p11.2^{flx}* mice expressing DIO-ChR2 in DR with either vehicle (black) or NAS-181 (blue) infused into the NAc before behaviour assays. Data are mean \pm s.e.m. * $P < 0.05$; repeated measures, two-way ANOVA with Tukey's multiple comparison post hoc test. Comparisons with no asterisk had $P > 0.05$ and were considered not significant.

5-HT1b Agonist: NAc Infusion



Extended Data Fig. 11 | See next page for caption.

Extended Data Fig. 11 | Infusion of 5-HT1b receptor agonist into the NAc increases sociability, but does not alter control behaviours.

a, Schematic of 5-HT1b receptor agonist (CP93129) infusion into the NAc in *Sert-cre* or *Sert-cre:16p11.2^{flx}* mice. **b**, Timeline of behavioural experiments. **c, d**, Quantification of chamber and proximity time in the three-chamber assay (**c**: vehicle, $F_{2,15} = 45.82$, $P < 0.001$ (left); $F_{3,30} = 4.453$, $P < 0.05$ (right), $n = 6$; **d**: CP93129, $F_{2,15} = 63.11$, $P < 0.001$ (left); $F_{1,10} = 17.23$, $P < 0.05$, (right), $n = 6$) in *Sert-cre* mice with either vehicle (red) or CP93129 (aqua) infused into the NAc before analysis of behaviour. **e, f**, Quantification of chamber and proximity time in the three-chamber assay (**e**: vehicle, $F_{2,12} = 67.49$, $P < 0.001$ (left); $F_{1,8} = 41.03$, $P < 0.001$ (right), $n = 5$; **f**: CP93129, $F_{2,12} = 29.73$, $P < 0.001$ (left); $F_{1,8} = 17.17$,

$P < 0.01$ (right), $n = 5$) in *Sert-cre:16p11.2^{flx}* mice with either vehicle (blue) or CP93129 (pink) infused into the NAc before analysis of behaviour. **g–i**, Quantification of the novel object interaction assay (**g**: $F_{1,18} = 1.612$, $P = 0.2204$, $n = 5–6$), locomotion assay (**h**: $F_{1,18} = 0.0149$, $P = 0.9041$, $n = 5–6$), and centre time (**i**: $F_{5,50} = 1.492$, $P = 0.2093$; $F_{5,40} = 0.4561$, $P = 0.8063$, $n = 5–6$) in *Sert-cre* and *Sert-cre:16p11.2^{flx}* mice with either vehicle or NAS-181 infused into the NAc before behaviour. Data are mean \pm s.e.m. * $P < 0.05$, ** $P < 0.01$, *** $P < 0.001$; repeated measures, two-way ANOVA with Tukey's multiple comparison post hoc test. Comparisons with no asterisk had $P > 0.05$ and were considered not significant. The schematic of the mouse brain in this figure has been adapted with permission from Franklin & Paxinos⁴⁶.

Life Sciences Reporting Summary

Nature Research wishes to improve the reproducibility of the work that we publish. This form is intended for publication with all accepted life science papers and provides structure for consistency and transparency in reporting. Every life science submission will use this form; some list items might not apply to an individual manuscript, but all fields must be completed for clarity.

For further information on the points included in this form, see [Reporting Life Sciences Research](#). For further information on Nature Research policies, including our [data availability policy](#), see [Authors & Referees](#) and the [Editorial Policy Checklist](#).

► Experimental design

1. Sample size

Describe how sample size was determined.

No statistical methods were used to predetermine sample sizes, which were based on work in previous publications (refs. Dolen, et al., 2013; Gunaydin, et al., 2014). Sample size of 5–15 animals were sufficient to determine significance both in behavior tests and electrophysiological recordings.

2. Data exclusions

Describe any data exclusions.

Out of the greater than 400 animals used in our experiments, <3% were excluded after euthanasia because of lack of detectable transgene expression in the targeted brain region.

3. Replication

Describe whether the experimental findings were reliably reproduced.

All attempts at replication were successful.

4. Randomization

Describe how samples/organisms/participants were allocated into experimental groups.

Animals were randomized by cage prior to surgeries. For example, if there were 30 mice in an experiment, with five mice per cage, mice were randomly assigned to be in eYFP or ChR2 groups in a counterbalanced fashion.

5. Blinding

Describe whether the investigators were blinded to group allocation during data collection and/or analysis.

All experiments were conducted in a blind manner such that assays were conducted and analyzed without knowledge of the specific manipulation being performed or the genotype of the animal being studied.

Note: all studies involving animals and/or human research participants must disclose whether blinding and randomization were used.

6. Statistical parameters

For all figures and tables that use statistical methods, confirm that the following items are present in relevant figure legends (or in the Methods section if additional space is needed).

n/a Confirmed

- The exact sample size (n) for each experimental group/condition, given as a discrete number and unit of measurement (animals, litters, cultures, etc.)
- A description of how samples were collected, noting whether measurements were taken from distinct samples or whether the same sample was measured repeatedly
- A statement indicating how many times each experiment was replicated
- The statistical test(s) used and whether they are one- or two-sided (note: only common tests should be described solely by name; more complex techniques should be described in the Methods section)
- A description of any assumptions or corrections, such as an adjustment for multiple comparisons
- The test results (e.g. P values) given as exact values whenever possible and with confidence intervals noted
- A clear description of statistics including central tendency (e.g. median, mean) and variation (e.g. standard deviation, interquartile range)
- Clearly defined error bars

See the web collection on [statistics for biologists](#) for further resources and guidance.

► Software

Policy information about [availability of computer code](#)

7. Software

Describe the software used to analyze the data in this study.

Behavioral experiments were assayed automatically using the video tracking system (BIOBSERVE, Version 3.01). Axograph X was used for the acquisition and analysis of electrophysiological recordings. Fiber photometry data was acquired with Synapse software controlling an RZ5P lock-in amplifier (Tucker-Davis Technologies). Signal processing was performed with Matlab (Mathworks, Inc.).

For manuscripts utilizing custom algorithms or software that are central to the paper but not yet described in the published literature, software must be made available to editors and reviewers upon request. We strongly encourage code deposition in a community repository (e.g. GitHub). *Nature Methods* [guidance for providing algorithms and software for publication](#) provides further information on this topic.

► Materials and reagents

Policy information about [availability of materials](#)

8. Materials availability

Indicate whether there are restrictions on availability of unique materials or if these materials are only available for distribution by a for-profit company.

All unique materials used are readily available from the authors or from standard commercial sources.

9. Antibodies

Describe the antibodies used and how they were validated for use in the system under study (i.e. assay and species).

No antibodies were used.

10. Eukaryotic cell lines

a. State the source of each eukaryotic cell line used.

No eukaryotic cells lines were used.

b. Describe the method of cell line authentication used.

No eukaryotic cells lines were used.

c. Report whether the cell lines were tested for mycoplasma contamination.

No eukaryotic cells lines were used.

d. If any of the cell lines used are listed in the database of commonly misidentified cell lines maintained by [ICLAC](#), provide a scientific rationale for their use.

No commonly misidentified cell lines were used.

► Animals and human research participants

Policy information about [studies involving animals](#); when reporting animal research, follow the [ARRIVE guidelines](#)

11. Description of research animals

Provide details on animals and/or animal-derived materials used in the study.

Male 7-9 week old C57Bl/6 mice (Jackson Laboratory), Tg(Slc6a4-cre)ET33Gsat (Sert-Cre, Jackson Laboratory), C57BL/6-Tg(Nes-cre/Esr1*)1Kuan/J (nestin-CreER, Jackson Laboratory), and B6N.129P2(Cg)-Igs13tm1Dolm Igs14tm1Dolm/J (16pll.2flx, gift from Ricardo Dolmetsch, Jackson Laboratory) were housed on a 12-hour light-dark cycle with food and water ad libitum. Mice were kept on a C57Bl/6 or CD-1 background.

Policy information about [studies involving human research participants](#)

12. Description of human research participants

Describe the covariate-relevant population characteristics of the human research participants.

The study did not involve human research participants.